JCB Journal of Cell Biology

ARTICLE

Cocaine-induced release of CXCL10 from pericytes regulates monocyte transmigration into the CNS

Fang Niu[1], Ke Liao[1], Guoku Hu[1], Susmita Sil[1], Shannon Callen[1], Ming-lei Guo[1], Lu Yang[2], and Shilpa Buch[1]

Cocaine is known to facilitate the transmigration of inflammatory leukocytes into the brain, an important mechanism underlying neuroinflammation. Pericytes are well-recognized as important constituents of the blood–brain barrier (BBB), playing a key role in maintaining barrier integrity. In the present study, we demonstrate for the first time that exposure of human brain vascular pericytes to cocaine results in enhanced secretion of CXCL10, leading, in turn, to increased monocyte transmigration across the BBB both in vitro and in vivo. This process involved translocation of σ-1 receptor (σ-1R) and interaction of σ-1R with c-Src kinase, leading to activation of the Src–PDGFR-β–NF-κB pathway. These findings imply a novel role for pericytes as a source of CXCL10 in the pericyte–monocyte cross talk in cocaine-mediated neuroinflammation, underpinning their role as active components of the innate immune responses.

Introduction

Cocaine use and its consequences continue to be a global epidemic. According to the World Drug Report, the number of cocaine users worldwide increased to 18.8 million in 2014 (United Nations Office on Drugs and Crime, 2016). Cocaine-related visits to hospital emergency departments remain a significant health care burden and accounted for ∼40.3% of all illegal drug-related emergency department visits in 2011 (Substance Abuse and Mental Health Services Administration, Center for Behavioral Health Statistics and Quality, 2013). Case reports indicate that cocaine use is often associated with seizures, cognitive impairment, depression, and an increased risk of stroke, all of which are major contributors to emergency department visits (Mendoza et al., 1992; Majlesi et al., 2010; Bodmer et al., 2014). Although the mechanisms underlying cocaine-associated central nervous system (CNS) disorders remain largely unknown, a variety of studies have implicated proinflammatory central immune signaling comprising both neuroexcitatory and neurotoxic effects as crucial factors in cocaine exposure/abuse (Rhoney, 2010; Fox et al., 2012; Li, 2016; Liao et al., 2016).

Monocytes are a subset of circulating white blood cells that can migrate across the blood–brain barrier (BBB) in pathological conditions and are implicated in the progression of many CNS neurodegenerative diseases, such as Alzheimer's disease, multiple sclerosis, Parkinson's disease, and human immunodeficiency virus (HIV)–associated neurocognitive disorders (Filion et al., 2003; Yao et al., 2010; Napuri et al., 2013; Grozdanov et al., 2014; Thériault et al., 2015). Intriguingly, cocaine has not only been found to enhance HIV-1 infectivity of monocyte-derived dendritic cells and macrophages (Dhillon et al., 2007), but also been shown to facilitate monocyte trafficking across the BBB, leading, in turn, to enhanced HIV disease progression and increased neuropathology (Yao et al., 2010, 2011b; Napuri et al., 2013; Dahal et al., 2015; Dash et al., 2015). The mechanisms by which cocaine elicits these responses, however, remain poorly understood.

Interstitial migration of monocytes is a dynamic, multistep process guided primarily by the local chemokine gradients that are formed by factors such as the C-C motif chemokine ligand 2 (CCL2), C-X3-C motif chemokine ligand 1, and C-X-C motif chemokine 10 (CXCL10; Taub et al., 1993; Yao et al., 2010; Pirvulescu et al., 2014). While CCL2 and C-X3-C motif chemokine ligand 1 have been widely linked with monocyte transmigration (Park et al., 2001; Butoi et al., 2011; Pirvulescu et al., 2014), studies of the role of CXCL10 in monocyte transmigration are limited. CXCL10, a proinflammatory chemokine produced by a variety of cell types including glia, dendritic cells, leukocytes, and endothelial cells (Taub et al., 1993; Vargas-Inchaustegui et al., 2010; Ioannidis et al., 2016), belongs to the CXCR3 (CD183) signaling family, including CXCL9/MIG (monokine-induced by γ-IFN), CXCL10/IP-10 (interferon inducible 10-kD protein) and CXCL11/I-TAC (inducible T cell-a chemoattractant). Elevated levels of CXCL10 have been associated with a variety of CNS diseases and viral infections such as tick-borne encephalitis, neuroborreliosis,

[1]Department of Pharmacology and Experimental Neuroscience, University of Nebraska Medical Center, Omaha, NE; [2]School of Medicine, University of Electronic Science and Technology of China, Chengdu, China.

Correspondence to Shilpa Buch: sbuch@unmc.edu.

https://doi.org/10.1083/jcb.201712011

Alzheimer's disease, multiple sclerosis, and HIV-associated neurocognitive disorders (Lepej et al., 2007; Zajkowska et al., 2011; Mehla et al., 2012; Simmons et al., 2013; Krauthausen et al., 2015). One study demonstrated increased plasma levels of CXCL10 in HIV-infected cocaine abusers compared with nonusers, thereby underscoring its role as a biomarker (Kamat et al., 2012). CXCL10 is a critical chemokine that is dramatically up-regulated in HIV-associated neuropathogenesis (Lane et al., 2003; Cinque et al., 2005) and other neurodegenerative diseases (Sørensen et al., 2001; Corrêa et al., 2011). In this study, we sought to inquire if cells in proximity to the BBB played a role in contributing to the increased CXCL10.

Pericytes are fundamental components of the microvascular vessel wall and play a vital role in the development and regulation of the BBB and vascular function; however, their role in neuroinflammation (Hall et al., 2014) has not been explored. The aim of the present study was to identify the role of pericytes in cocaine-mediated monocyte transmigration, and the molecular mechanisms by which cocaine induces secretion of CXCL10 from human brain pericytes. Understanding the regulation of CXCL10 expression by cocaine could provide insights into the development of therapeutic targets for cocaine-mediated neuroinflammation.

Results

Increased number of CD68$^+$ macrophages proximal to CXCL10 overexpressing pericytes in the brains of cocaine abusers

In this study, we sought to assess the frontal cortices of postmortem brain tissues from no-cocaine controls and cocaine abusers for the presence of CD68$^+$ (macrophage marker)/TMEM119$^-$ (resident microglial marker) cells in proximity of Desmin$^+$ pericytes. We found an increased number of CD68$^+$/TMEM119$^-$ cells accumulated around Desmin$^+$ pericytes in brains of cocaine abusers compared with no-cocaine controls (Fig. 1 A). There was an increased number of CD68$^+$/TMEM119$^-$ cells in proximity to Desmin$^+$ pericytes (Fig. 1 B). To understand the role of CXCL10 in pericyte–monocyte cross talk, we next sought to examine the expression of CXCL10 in the microvessels (MIVs) isolated from the frontal cortices of postmortem brain tissues from no-cocaine controls as well as cocaine abusers. MIVs were costained with anti-CXCL10 and the pericyte markers PDGF receptor-β (PDGFR-β), NG2, Desmin, or TBX18 as well as the endothelial cell marker CD31. There was increased CXCL10 expression in the pericyte marker PDGFR-β–positive cells in the MIVs isolated from cocaine abusers compared with no-cocaine controls (Fig. 1 C). Quantification of CXCL10 fluorescent intensity in PDGFR-β$^+$ cells is shown in Fig. 1 D. Increased expression of CXCL10 was also observed in NG2$^+$, Desmin$^+$, and TBX18$^+$ pericytes in MIVs of cocaine abusers, compared with no-cocaine controls (Fig. 1, E–J).

Cocaine-mediated enhanced expression and mRNA stability of CXCL10 in human brain vascular pericytes (HBVPs)

Based on the findings that in the brains of cocaine abusers, increased expression of CXCL10 was closely associated with enhanced monocyte transmigration, we next sought to determine the effect of cocaine exposure on the expression of CXCL10 in HBVPs. We first assessed dose and time course of CXCL10 expression following exposure of HBVPs to cocaine. For the dose curve, HBVPs were treated with varying concentrations (10^{-8}, 10^{-7}, 10^{-6}, 10^{-5}, and 10^{-4} M) of cocaine for 1 h, followed by assessment of CXCL10 mRNA by real-time PCR. In HBVPs, cocaine up-regulated expression of CXCL10 in a dose-dependent manner with a maximal response at 10^{-5} M (10 µM; 2.9-fold, P = 0.0049; Fig. 2 A). This concentration of cocaine was therefore used for all further experiments; physiologically relevant concentrations of cocaine found in the plasma of human cocaine addicts range from 0.4–13 µM (Stephens et al., 2004). All the cocaine concentrations tested failed to exert any toxicity on HBVPs, as determined by a cell viability assay (Fig. S1 C).

For the time-course study, HBVPs were exposed to cocaine (10 µM) for various time periods (1–24 h) followed by assessment of CXCL10 mRNA by real-time PCR. In HBVPs exposed to 10 µM cocaine, there was maximal induction of CXCL10 expression at 1 h (2.6-fold, P < 0.0001) with a drop in expression thereafter that persisted up to 3 h (Fig. 2 B). To validate the specificity of cocaine-mediated induction of CXCL10 in pericytes, we also assessed the effect of cocaine in another unrelated cell line—HEK293 cells. HEK293 cells were exposed to cocaine (10 µM) for various time periods (1–24 h) and assessed for the expression of CXCL10 mRNA by real-time PCR. As shown in Fig. S2 A and unlike the pericytes, cocaine exposure failed to up-regulate CXCL10 mRNA expression in HEK293 cells.

We next sought to determine whether cocaine-mediated induction of CXCL10 was regulated transcriptionally. For this we used six CXCL10 promoter–luciferase constructs reported previously by Dr. David Proud (University of Calgary, Calgary, Alberta, Canada; Koetzler et al., 2009)—the 972-bp full-length CXCL10 promoter (IFN-γ–inducible protein of pGL4), the 376-bp truncated CXCL10 promoter, and the CXCL10 promoter with point mutations in the activator protein-1 (AP-1), NF-κB1 (κB1), NF-κB2 (κB2), and IFN-stimulated response element (ISRE) recognition elements in the 972-bp full-length promoter. Herein, HBVPs were cotransfected with each of the indicated promoter plasmids described above, as well as with a *Renilla* luciferase–expressing plasmid. Following transfection, HBVPs were treated with cocaine, and promoter activity was assessed by monitoring relative luciferase activities using the Dual-Luciferase reporter 1000 assay system. Cocaine exposure resulted in significant activation of both full-length and truncated promoter luciferase constructs, with similar induction of luciferase activity by both the constructs (Fig. 2 C; 1.33-fold, P = 0.0446; 1.37-fold, P = 0.0408). Based on this result, it was inferred that the key promoter elements crucial for cocaine-mediated induction of CXCL10 transcription were contained within the 376-bp promoter, including AP-1, κB1, κB2, and ISRE recognition elements. To dissect the potential transcription factor binding sites engaged by cocaine on the CXCL10 promoter, the next step was to assess the ability of cocaine to induce/abrogate CXCL10 transcription in cells transfected with constructs containing various point mutations (AP-1, κB1, κB2, and ISRE recognition elements) in the full-length CXCL10 promoter. Mutations in the AP-1 site had no significant effect on the ability of cocaine to induce promoter activation (Fig. 2 C); however, mutations in the κB1, κB2, and ISRE sites all

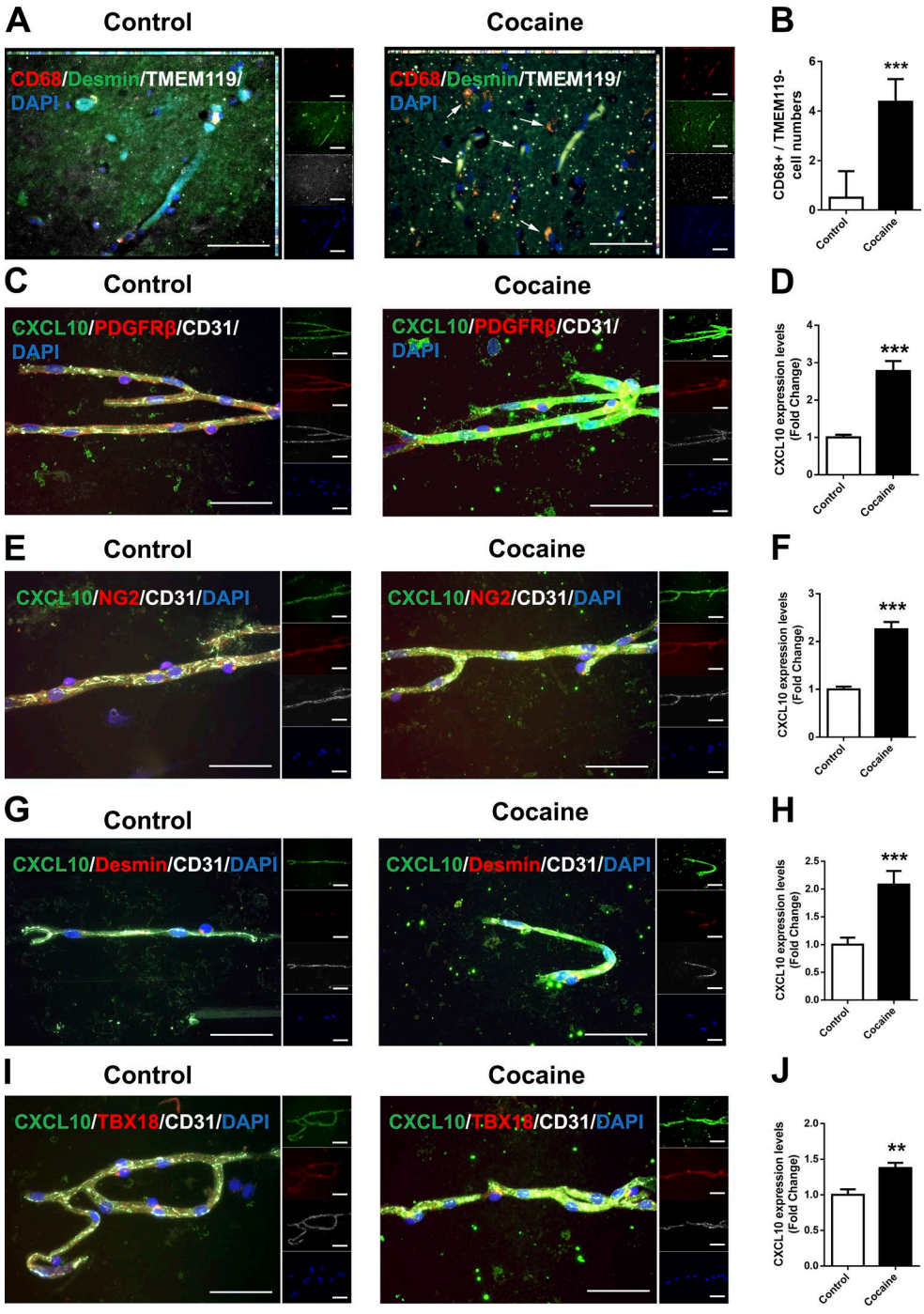

Figure 1. **Increased numbers of CD68⁺ macrophages proximal to CXCL10 overexpressing pericytes in the brains of cocaine abusers. (A)** Representative immunostaining of the frontal cortex region from the postmortem brain tissues of no-cocaine controls or cocaine users stained with anti-CD68 (macrophage marker, red), anti-Desmin (pericyte marker, green), and anti-TMEM119 (resident microglial marker, white) antibodies. *n* = 4 per group; bar, 50 µm. Arrows: CD68⁺/TMEM119⁻ cells. **(B)** Quantification of CD68⁺/TMEM119⁻ cells in the frontal cortex region of no-cocaine controls or cocaine users. Two-tailed Student's *t* test. **(C)** Representative images of MIVs isolated from the frontal cortices of no-cocaine controls or cocaine abusers that were stained with anti-CXCL10, anti–PDGFR-β, and anti-CD31 antibodies. *n* = 4 per group; bar, 50 µm. **(D)** Quantification of fluorescent intensities of CXCL10 staining in PDGFR-β⁺ cells. Two-tailed Student's *t* test. **(E)** Representative images of MIVs isolated from the frontal cortices of no-cocaine controls or cocaine abusers that were stained with anti-CXCL10, anti-NG2, and anti-CD31 antibodies. *n* = 4 per group; bar, 50 µm. **(F)** Quantification of fluorescent intensities of CXCL10 staining in NG2⁺ cells. Two-tailed Student's *t* test. **(G)** Representative images of MIVs isolated from the frontal cortices of no-cocaine controls or cocaine abusers that were stained with anti-CXCL10, anti-Desmin, and anti-CD31 antibodies. *n* = 4 per group; bar, 50 µm. **(H)** Quantification of fluorescent intensities of CXCL10 staining in Desmin⁺ cells. Two-tailed Student's *t* test. **(I)** Representative images of MIVs isolated from the frontal cortices of no-cocaine controls or cocaine abusers that were stained with anti-CXCL10, anti-TBX18, and anti-CD31 antibodies. *n* = 4 per group; bar, 50 µm. **(J)** Quantification of fluorescent intensities of CXCL10 staining in TBX18⁺ cells. All data are presented as means ± SD of three or four individual experiments (biological replicates). **, P < 0.01, ***, P < 0.001 versus control group.

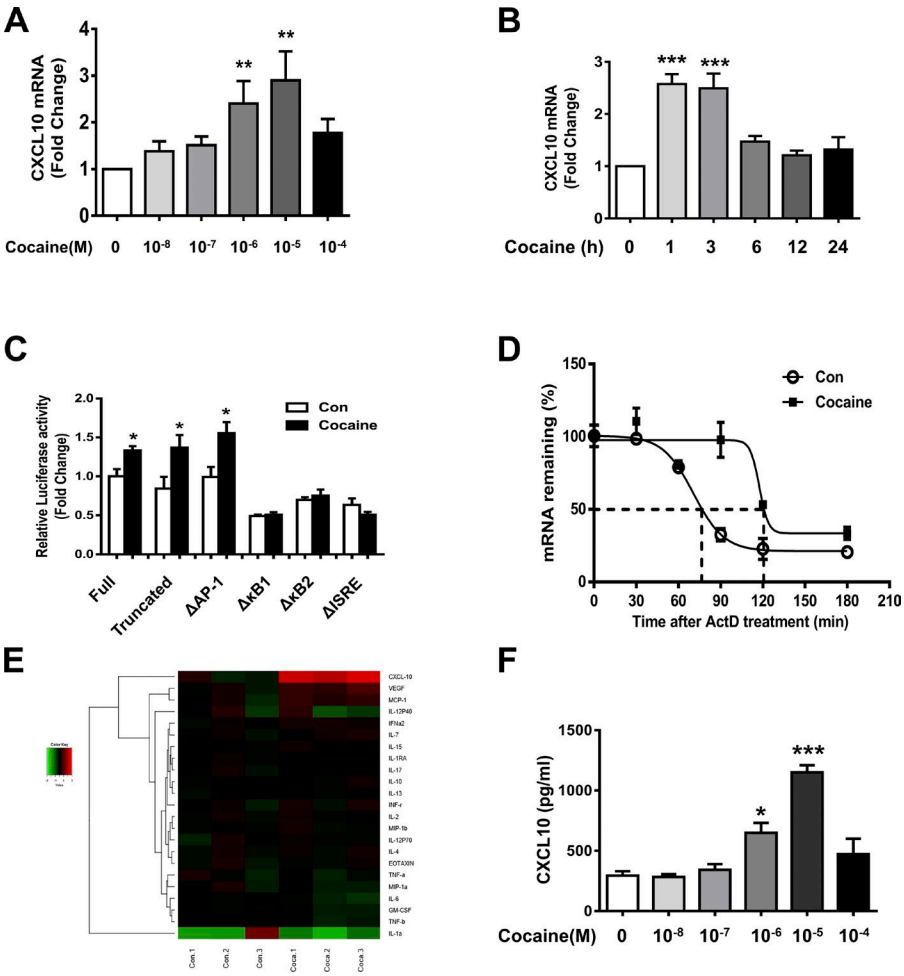

Figure 2. **Cocaine enhanced mRNA stability and expression of CXCL10 in HBVPs. (A)** Real-time PCR analysis of CXCL10 mRNA expression in HBVPs exposed to varying concentrations of cocaine (10^{-8}, 10^{-7}, 10^{-6}, 10^{-5}, and 10^{-4} M). One-way ANOVA followed by Bonferroni's post hoc test was used to determine the statistical significance among multiple groups. **(B)** Real-time PCR analysis of CXCL10 mRNA expression in HBVPs exposed to cocaine (10 µM) for various time points. One-way ANOVA followed by Bonferroni's post hoc test was used to determine the statistical significance among multiple groups. **(C)** HBVPs were transfected with luciferase reporter gene constructs containing either full-length or truncated CXCL10 promoter for 24 h followed by stimulation with cocaine for an additional 4 h. Two-tailed Student's *t* test. **(D)** Kinetics of CXCL10 mRNA expression by real-time PCR in both control and cocaine-stimulated HBVPs in the presence of Act D. **(E)** Heatmap representing expression levels of cytokines/chemokines in the supernatant of control and cocaine exposed HBVPs. **(F)** CXCL10 was assayed by ELISA in supernatants of HBVPs cultured for 24 h in the absence or presence of cocaine. One-way ANOVA followed by Bonferroni's post hoc test was used to determine the statistical significance among multiple groups. All data are presented as means ± SD or SEM of three or four individual experiments (biological replicates). *, P < 0.05, **, P < 0.01, ***, P < 0.001 versus control group.

led to significant abrogation of cocaine-induced luciferase activity, thereby underscoring the role of these transcription factor binding sites in cocaine-mediated induction of CXCL10.

Since CXCL10 mRNA expression following cocaine exposure increased 2.9-fold in HBVPs, whereas the transcriptional activation only increased 1.33-fold, we hypothesized that the induction of CXCL10 mRNA by cocaine could be mediated, in part, by an increase in CXCL10 mRNA stability. To assess this, HBVPs were treated with actinomycin D (Act D; 10 µg/ml) in the presence or absence of cocaine for various time periods (30–180 min) to block the de novo mRNA synthesis, followed by assessment of CXCL10 mRNA levels by quantitative PCR. Cocaine exposure resulted in an increased half-life of CXCL10 mRNA ($t_{1/2}$ = 120 min) compared with the control group ($t_{1/2}$ = 77 min; Fig. 2 D).

To confirm whether increased CXCL10 mRNA levels manifested as increased protein translation, HBVPs were treated with 10 µM cocaine for 24 h followed by collection of supernatants that were assessed for a panel of cytokines/chemokines using the Luminex platform. As shown in the heatmap (Fig. 2 E), protein expression of CXCL10, VEGF, and CCL2 was significantly induced by cocaine in HBVPs compared with the unexposed controls (CXCL10: 5.19-fold, P = 0.000985; VEGF: 1.63-fold, P = 0.0289; CCL2: 1.46-fold, P = 0.0430); moreover, CXCL10 was the most prominently expressed chemokine among all 23 detectable chemokines. Out of a panel of 29 cytokines/chemokines, we were able to detect 23 cytokines/chemokines in our system. To validate our Luminex assay findings, HBVPs were treated with cocaine at varying concentrations (10^{-8}, 10^{-7}, 10^{-6}, 10^{-5}, and 10^{-4} M) for 24 h, followed by collection of supernatants that were assessed for expression of secreted CXCL10 using the ELISA assay. Similar to our Luminex results, cocaine induced CXCL10 release from HBVPs in a concentration-dependent manner with maximal response at 10^{-5} M (10 µM; 1,151 pg/ml, P < 0.0001) as determined by ELISA (Fig. 2 F). Taken together, these findings suggest that in HBVPs, cocaine mediated induction and release of CXCL10 by increasing the transcriptional activity, as well as mRNA stability of CXCL10 mRNA.

Engagement of σ-1 receptor (σ-1R) is critical for cocaine-mediated induction of CXCL10 expression in HBVPs

Since σ-1R is known to bind to a plethora of psychotropic drugs including cocaine (Hayashi and Su, 2003), we next sought to determine whether σ-1R was involved in cocaine-mediated induction of CXCL10 release from HBVPs. The first step was to examine the endogenous expression of σ-1R in HBVPs by RT-PCR. Basal expression level of σ-1R in HBVPs was lower compared with human brain microvascular endothelial cells (HBMECs; Fig. 3 A). Next, we sought to determine whether activation of σ-1R by cocaine involved translocation of these receptors from the ER lipid droplets to the plasma membrane. For this, we first isolated lipid

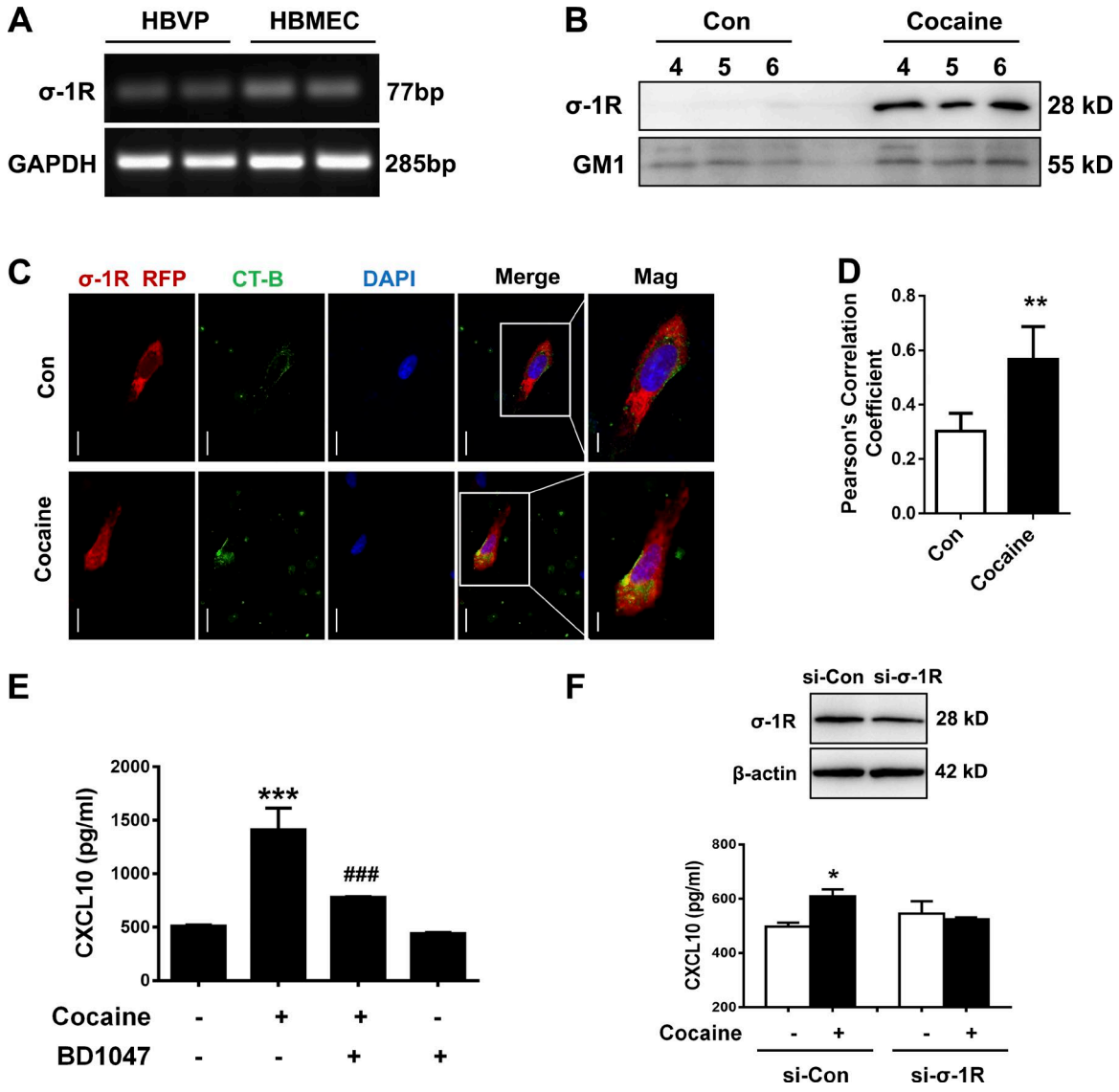

Figure 3. **Engagement of σ-1R is critical for cocaine-induced CXCL10 expression in HBVPs. (A)** Comparative expression of σ-1R mRNA levels by RT-PCR analysis in both HBVPs and HBMECs. **(B)** Representative Western blot of σ-1R and GM1 in the lipid raft fractions (4–6) isolated from confluent HBVPs either unexposed or exposed to cocaine using sucrose gradient ultracentrifugation. **(C)** Representative fluorescence images of HBVPs transfected with σ-1R–RFP plasmid (red fluorescence) and stained with CT-B conjugates Alexa Fluor 488 specific for ganglioside GM1-lipid raft marker (green fluorescence). Bar, 10 µm. Overlay and magnified (mag) images are shown; bar, 5 µm. **(D)** Quantification of colocalization of σ-1R and CT-B. Two-tailed Student's *t* test. **(E)** CXCL10 was assayed by ELISA assay in the supernatants collected from HBVPs pretreated with σ-1R inhibitor BD1047 (10 µM) for 1 h, followed by cocaine exposure for an additional 24 h. One-way ANOVA followed by Bonferroni's post hoc test was used to determine the statistical significance among multiple groups. **(F)** Representative Western blot of silencing of σ-1R in HBVPs transfected with si–σ-1R. CXCL10 was assayed by ELISA assay in the supernatants collected from HBVPs transfected with si–σ-1R and nonsense si-Con followed by cocaine exposure. One-way ANOVA followed by Bonferroni's post hoc test was used to determine the statistical significance among multiple groups. All data are presented as means ± SD of three or four individual experiments (biological replicates). *, P < 0.05, **, P < 0.01, ***, P < 0.001 versus control group. ###, P < 0.001 versus cocaine-exposed group.

rafts from HBVPs by sucrose gradient centrifugation and examined each fraction for the expression of σ-1R and GM1 by Western blot (Fig. 3 B). σ-1Rs were primarily present in fractions 8–10, while GM1 gangliosides were primarily present in fractions 4 and 5. Next, HBVPs were exposed to cocaine (10 µM) for 20 min, followed by lipid raft isolation and assessment of σ-1R and GM1 in fractions 4–6 by Western blot. Following cocaine exposure, there was a significant increase in σ-1R expression in the lipid raft fractions from HBVPs compared with controls (Fig. 3; expression of σ-1R in all the 10 fractions is shown in Fig. S2 B).

These findings were also validated by immunostaining of HBVP cells transfected with the σ-1R RFP plasmid. HBVPs were transfected with the σ-1R RFP plasmid for 24 h, exposed to cocaine for 15 min, followed by GM1 staining with Alexa-conjugated cholera toxin subunit B (CT-B), and assessed by fluorescence microscopy. In untreated control HBVPs, σ-1R (red) was mainly expressed in the cytoplasm and failed to colocalize with the lipid raft microdomains (Fig. 3 C, green). After cocaine exposure, however, there was colocalization of σ-1R within the lipid raft domains as evidenced by merging of green and red staining. This

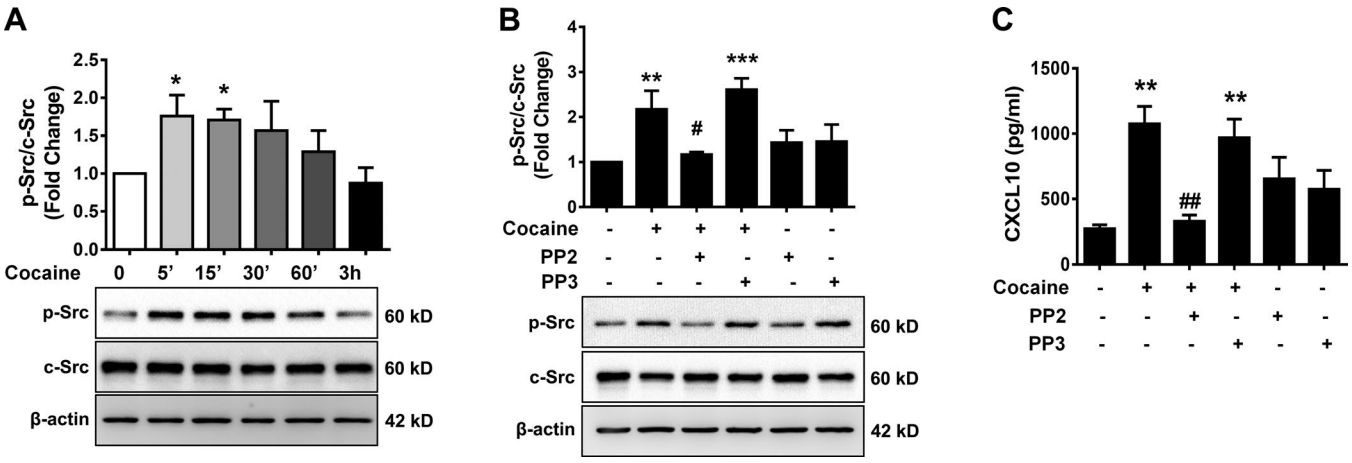

Figure 4. **Involvement of c-Src kinase in cocaine-mediated CXCL10 expression. (A)** Representative Western blot and quantification of p-Src and c-Src in the lysates isolated from HBVPs exposed to cocaine for various time points (5 min to 3 h). One-way ANOVA followed by Bonferroni's post hoc test was used to determine the statistical significance among multiple groups. **(B)** Representative Western blot and quantification of p-Src and c-Src in the lysates isolated from HBVPs pretreated with Src tyrosine kinase inhibitor PP2 (1 µM) or its inactive analogue PP3 (1 µM) for 1 h, followed by cocaine exposure for an additional 15 min. One-way ANOVA followed by Bonferroni's post hoc test was used to determine the statistical significance among multiple groups. **(C)** CXCL10 was assayed by ELISA assay in the supernatants collected from HBVPs pretreated with either the Src tyrosine kinase inhibitor PP2 or its inactive analogue PP3 for 1 h, followed by cocaine exposure for an additional 24 h. One-way ANOVA followed by Bonferroni's post hoc test was used to determine the statistical significance among multiple groups. All data are presented as means ± SD of four or five individual experiments (biological replicates). *, P < 0.05, **, P < 0.01, ***, P < 0.001 versus control group. #, P < 0.05, ##, P < 0.01 versus cocaine-treated group.

observation was quantified using Pearson's correlation coefficient (Fig. 3 D).

Having determined that cocaine activated σ-1R via its translocation into the lipid domains of plasma membrane, we next sought to examine the role of σ-1R in cocaine-mediated induction of CXCL10 in HBVPs. Cocaine-mediated induction of CXCL10 expression was significantly attenuated in HBVPs pretreated with the σ-1R antagonist BD1047 (10 µM; Fig. 3 E). To further validate the involvement of σ-1R in cocaine-induced regulation of CXCL10 expression, we used a genetic knockdown approach by transfecting HBVPs with σ-1R siRNA (si–σ-1R). Transfection of HBVPs with si–σ-1R resulted in efficient knockdown of σ-1R expression (Fig. 3 F). In cells transfected with si–σ-1R, cocaine failed to up-regulate the expression of CXCL10 compared with cells transfected with scrambled siRNA. These findings thus underscore the role of σ-1R in cocaine-mediated induction of CXCL10 in HBVPs.

Involvement of c-Src kinase in cocaine-mediated induction of CXCL10 in HBVPs

We next sought to examine whether cocaine-mediated induction of CXCL10 involved activation of c-Src. Exposure of HBVPs to cocaine resulted in a time-dependent increase in phosphorylation of c-Src, with activation as early as 5 min following exposure (Fig. 4 A). The specificity of Src signaling pathway was subsequently assessed using a pharmacological approach. Pretreatment of cells with the Src tyrosine kinase inhibitor PP2 resulted in abrogation of cocaine-induced phosphorylation of c-Src (Fig. 4 B). As expected, pretreatment of cells with the inactive analogue PP3 failed to abrogate cocaine-induced phosphorylation of c-Src. To examine the functional role of c-Src in cocaine-mediated induction of CXCL10 expression, HBVPs were pretreated with PP2 or PP3 for 1 h, followed by exposure of cells to cocaine for 24 h, followed by assessment of CXCL10 secretion by ELISA. Pretreatment of cells with PP2, not with PP3, significantly inhibited cocaine-mediated induction of CXCL10 secretion (Fig. 4 C).

Physical interaction of σ-1R with Src kinase

Since σ-1R translocated to the lipid raft domain in the membrane following exposure to cocaine, we sought to determine the presence of any protein–protein interactions between σ-1R and c-Src kinase. First, a series of coimmunoprecipitation assays was performed using lysates from cocaine-treated/nontreated HBVPs. In HBVPs, the amount of σ-1R in the c-Src–immunoprecipitated protein complex was increased following cocaine exposure, while the amount of total c-Src remained unchanged (Fig. 5 A). These findings allude to a possible interaction between σ-1R and c-Src kinase following cocaine exposure. For additional validation of this interaction, σ-1R was immunoprecipitated from HBVP lysates and assessed for expression of c-Src by Western blot. Similar to the c-Src immunoprecipitated complex, the amount of c-Src in the σ-1R–immunoprecipitated protein complex was increased following cocaine exposure, while the amount of total σ-1R remained unchanged.

The protein–protein interaction between σ-1R and c-Src was further validated by confocal microscopy. HEK293 cells were cotransfected with c-Src–GFP and σ-1R–RFP and assessed for colocalization of c-Src and σ-1R by confocal microscopy. As expected, c-Src and σ-1R were found in the cytoplasm of HEK293 cells with strong colocalization (yellow) of green and red fluorescence observed within the cells, demonstrating an interaction of c-Src with σ-1R (Fig. 5 B).

Since p-Src is the active form of c-Src (Rutledge et al., 2014), we next examined the interaction of p-Src with σ-1R in HBVPs. HBVPs were treated with cocaine (10 µM) for 15 min followed by assessment of p-Src (green color) and σ-1R (red color) by double

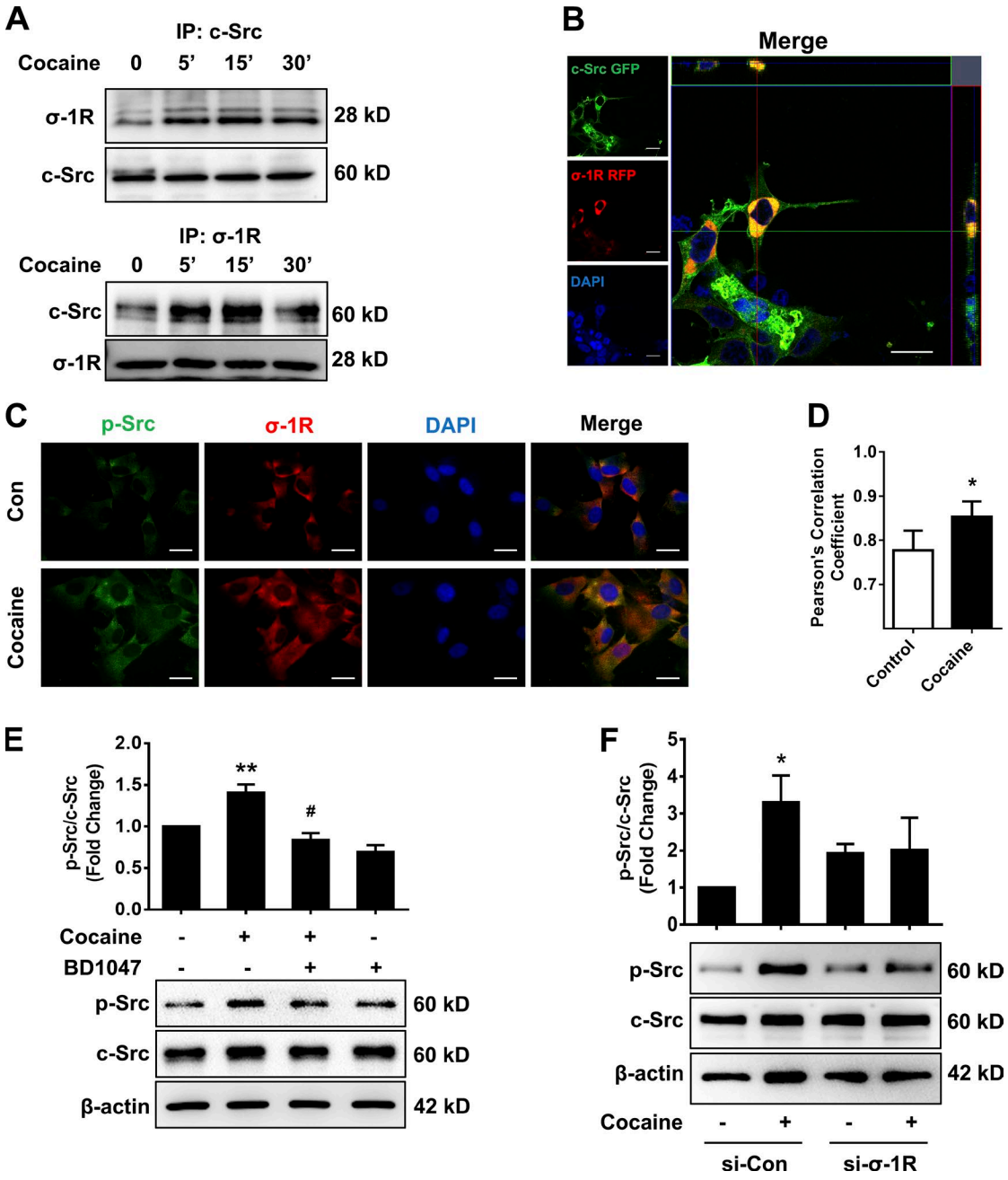

Figure 5. **Physical interaction of σ-1R with c-Src kinase. (A)** Cocaine mediated an interaction between σ-1R and c-Src, as determined by coimmunoprecipitation assay. **(B)** HEK293 cells were transfected with GFP-tagged c-Src and σ-1R–RFP. Overlay images are shown. Bar, 10 µm. **(C)** Representative fluorescence images of HBVPs stained with anti–p-Src (green) and σ-1R (red). Bars, 10 µm. **(D)** Quantification of colocalization of σ-1R and p-Src. Two-tailed Student's *t* test. **(E)** Representative Western blot and quantification of p-Src and c-Src in the lysates isolated from HBVPs pretreated with σ-1R inhibitor BD1047 (10 µM) for 1 h, followed by cocaine exposure for an additional 15 min. One-way ANOVA followed by Bonferroni's post hoc test was used to determine the statistical significance among multiple groups. **(F)** Representative Western blot and quantification of p-Src and c-Src in the lysates isolated from HBVPs transfection with si–σ-1R and si-Con followed by cocaine exposure for 15 min. One-way ANOVA followed by Bonferroni's post hoc test was used to determine the statistical significance among multiple groups. All data are presented as means ± SD or SEM of four or five individual experiments (biological replicates). *, P < 0.05, **, P < 0.01 versus control group. #, P < 0.05 versus cocaine-treated group.

immunostaining. The intensity of p-Src fluorescence and the colocalization of p-Src and σ-1R were both dramatically induced following cocaine exposure in HBVPs compared with control cells (Fig. 5 C). This finding was quantified using Pearson's correlation coefficient and shown in Fig. 5 D.

We next wanted to investigate whether activation of σ-1R was critical for cocaine-mediated phosphorylation of c-Src. Cocaine-mediated phosphorylation of c-Src was significantly attenuated in HBVPs pretreated with the σ-1R antagonist BD1047 (10 µM; Fig. 5 E). Similarly, transfection of HBVPs with σ-1R siRNA further validated the involvement of σ-1R in cocaine-induced phosphorylation of c-Src. In cells transfected with σ-1R siRNA, cocaine failed to mediate phosphorylation of c-Src, unlike the cells transfected with scrambled siRNA (Fig. 5 F). These

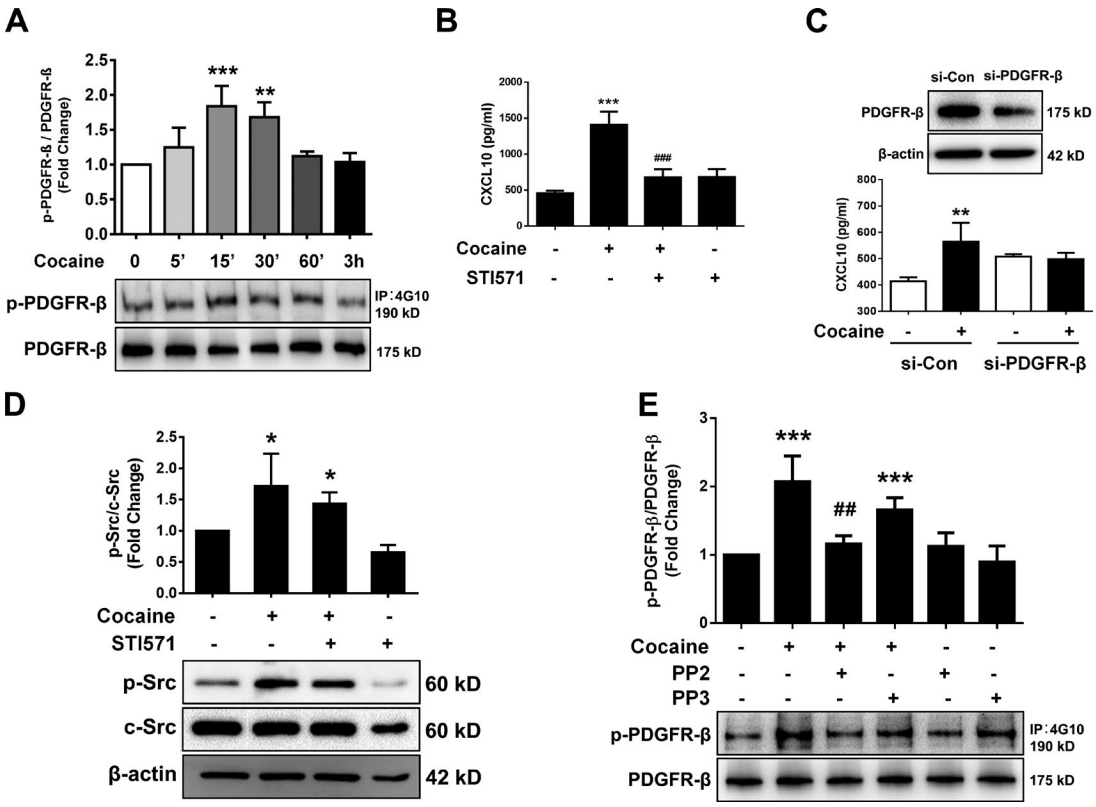

Figure 6. **Involvement of PDGFR-β in cocaine-mediated induction of CXCL10 expression. (A)** Phosphorylation of PDGFR-β induced by cocaine in HBVPs. One-way ANOVA followed by Bonferroni's post hoc test was used to determine the statistical significance among multiple groups. **(B)** CXCL10 was assayed by ELISA assay in the supernatants collected from HBVPs pretreated with the tyrosine kinase inhibitor STI571 (10 µM) for 1 h, followed by cocaine exposure for an additional 24 h. One-way ANOVA followed by Bonferroni's post hoc test was used to determine the statistical significance among multiple groups. **(C)** Representative Western blot of silencing of PDGFR-β in HBVPs transfected with si–PDGFR-β. CXCL10 was assayed by ELISA assay in the supernatants collected from HBVPs transfected with si–PDGFR-β and control siRNA followed by cocaine (10 µm) exposure for 24 h. One-way ANOVA followed by Bonferroni's post hoc test was used to determine the statistical significance among multiple groups. **(D)** Representative Western blot and quantification of p-Src and c-Src in the lysates isolated from HBVPs pretreated with the tyrosine kinase inhibitor STI571 for 1 h, followed by cocaine exposure for an additional 15 min. One-way ANOVA followed by Bonferroni's post hoc test was used to determine the statistical significance among multiple groups. **(E)** Representative Western blot and quantification of p-PDGFR-β/PDGFR-β in the lysates isolated from HBVPs pretreated with Src tyrosine kinase inhibitor PP2 or its inactive analogue PP3 for 1 h, followed by cocaine exposure for an additional 15 min. One-way ANOVA followed by Bonferroni's post hoc test was used to determine the statistical significance among multiple groups. All data are presented as means ± SD of four or five individual experiments (biological replicates). *, P < 0.05, **, P < 0.01, ***, P < 0.001 versus control group. ##, P < 0.01 versus cocaine-treated group.

findings thus demonstrate that cocaine-mediated activation of σ-1R is upstream of phosphorylation of c-Src.

Involvement of PDGFR-β in cocaine-mediated induction of CXCL10 expression

Based on the premise that the activation of σ-1R and c-Src plays a role in cocaine-mediated induction of CXCL10, and the fact that Src kinases are important for PDGFR-β signaling transduction, the next step was to elucidate whether cocaine-mediated CXCL10 expression involved PDGFR-β signaling. For this, HBVPs were exposed to cocaine for various time periods (between 5 min and 3 h) followed by assessment of the cell lysates for phosphorylation of PDGFR-β by immunoprecipitation assay using the anti-phosphotyrosine antibody (clone 4G10). In HBVPs, cocaine exposure resulted in phosphorylation of PDGFR-β as early as 5 min (Fig. 6 A). We next sought to elucidate whether PDGFR-β activation played a role in cocaine-mediated induction of CXCL10 expression. To address this, HBVPs were pretreated with a tyrosine kinase inhibitor, STI571 (10 µM), followed by exposure of cells to cocaine and assessment of CXCL10 release by ELISA. Pretreatment of cells with STI571 resulted in significant amelioration of cocaine-mediated release of CXCL10 from HBVPs (Fig. 6 B). Further validation of the involvement of PDGFR-β in cocaine-mediated CXCL10 release from HBVPs was performed in cells transfected with the siRNA for PDGFR-β, followed by assessment of CXCL10 release by ELISA assay. Transfection of HBVPs with PDGFR-β siRNA (si–PDGFR-β) resulted in efficient knockdown of PDGFR-β expression (Fig. 6 C). In these cells, cocaine failed to up-regulate CXCL10 release from HBVPs compared with HBVPs transfected with scrambled siRNA (si-Con), wherein, as expected, cocaine exposure up-regulated the expression of CXCL10.

The next step was to elucidate the role of c-Src in cocaine-mediated phosphorylation of PDGFR-β in HBVPs. Briefly, before cocaine exposure, HBVPs were pretreated with the tyrosine kinase inhibitor STI571 (10 µM) followed by assessment of phosphorylation of c-Src by Western blot. In cells pretreated with STI571, cocaine was able to induce phosphorylation of c-Src, demonstrating

thereby that c-Src was upstream of PDGFR-β signaling (Fig. 6 D). Reciprocally, HBVPs were also pretreated with the Src tyrosine kinase inhibitor PP2 or its inactive analogue PP3, followed by cocaine exposure and assessment of phosphorylation of PDGFR-β. In cells pretreated with PP2 but not PP3, cocaine-mediated phosphorylation of PDGFR-β was abrogated, thereby suggesting that c-Src lies upstream of PDGFR-β phosphorylation (Fig. 6 E).

Involvement of NF-κB in cocaine-mediated induction of CXCL10 expression

For further validation of the role of NF-κB, we next sought to examine the cocaine-mediated translocation of NF-κB p65 into the nucleus in HBVPs. Briefly, HBVPs were exposed to cocaine for various periods of time (5–180 min) and assessed for translocation of the p65 subunit of NF-κB into the nucleus. Exposure of HBVPs to cocaine resulted in a time-dependent increase in translocation of the NF-κB p65 subunit in the nucleus with a concomitant decrease in its expression in the cytosol (Fig. 7, A and B). Additional confirmation of these findings by immunostaining also revealed enhanced translocation of NF-κB into the nucleus in HBVPs at 15 min after cocaine (10 μM) exposure. Images were captured by fluorescence microscopy, using a (63×/1.4) objective lens. Cocaine exposure resulted in a significant increase in the intensity of NF-κB fluorescence in the nucleus with a concomitant decrease in the cytoplasm (Fig. 7 C). Quantification of NF-κB nuclear translocation is shown in Fig. 7 D. We next sought to examine whether NF-κB was involved in secretion of CXCL10. For this, HBVPs were pretreated with SC514, a selective IκB kinase-2 (IKK-2) inhibitor, to specifically suppress the transcription of NF-κB, followed by exposure to cocaine and assessment of CXCL10 release by ELISA. Pretreatment of cells with SC514 resulted in significant amelioration of cocaine-mediated CXCL10 release from HBVPs (Fig. 7 E).

To assess if there was a link that could tie together the activation of σ-1R–c-Src–PDGFR-β signaling with NF-κB, HBVPs were transfected with either nontarget siRNA control or si–σ-1R followed by exposure of transfected cells to cocaine for 15 min and assessment of NF-κB expression in the nuclear fraction. As expected, in HBVPs transfected with si–σ-1R, cocaine exposure failed to increase the nuclear translocation of NF-κB compared with cells transfected with the nontarget siRNA control, wherein cocaine exposure mediated increased translocation of NF-κB (Fig. 7 F). To examine the role of c-Src in cocaine-mediated nuclear translocation of NF-κB, HBVPs were pretreated with either the Src tyrosine kinase inhibitor PP2 or its inactive analogue PP3, followed by cocaine exposure. Pretreatment with PP2, but not with PP3, resulted in abrogation of cocaine-mediated nuclear translocation of NF-κB (Fig. 7 G). Having demonstrated the σ-1R and c-Src were involved in cocaine-mediated nuclear translocation of NF-κB, we next sought to examine the role of PDGFR-β in cocaine-induced NF-κB nuclear translocation. HBVPs were transfected with either nontarget siRNA control or si–PDGFR-β, followed by exposure of transfected cells to cocaine for 15 min, and assessed for expression of NF-κB in the nuclear fractions. Cocaine mediated an increase in translocation of NF-κB in cells transfected with the nontarget siRNA control but not in cells transfected with si–PDGFR-β (Fig. 7 H). These findings thus underpin the involvement of σ-1R–c-Src–PDGFR-β signaling in cocaine-mediated activation of NF-κB in HBVPs.

The next step was to examine a link between NF-κB activation and the upstream signaling pathways in cocaine-mediated up-regulation of CXCL10 expression in HBVPs. We thus first sought to assess whether pharmacological inhibition of NF-κB would affect cocaine-mediated translocation of σ-1R. For this, HBVPs were pretreated with SC514 for 1 h, then exposed to cocaine for an additional 15 min and assessed for translocation of σ-1R. In cells pretreated with SC514, cocaine was still able to induce translocation of σ-1R to the lipid rafts (Fig. S3, A and B). Next, we sought to examine whether inhibition of NF-κB could affect cocaine-mediated phosphorylation of c-Src. Briefly, HBVPs were pretreated with SC514 (10 μM) followed by assessing phosphorylation of c-Src by Western blots. In the presence of SC514, cocaine continued to mediate phosphorylation of c-Src (Fig. S3 C). We next assessed cocaine-mediated phosphorylation of PDGFR-β in the presence of SC514. HBVPs were pretreated with SC514, followed by cocaine exposure, and assessed for phosphorylation of PDGFR-β. In the presence of SC514, cocaine-mediated phosphorylation of PDGFR-β continued to persist (Fig. S3 D).

Cocaine-mediated release of CXCL10 from HBVPs facilitated monocyte transmigration in an in vitro BBB model

We next sought to determine whether cocaine-mediated up-regulation of released CXCL10 in HBVPs could induce monocyte transmigration. We used an in vitro BBB model to assess monocyte transmigration (Fig. 8 A). Briefly, HBMECs (4×10^4/well) were seeded onto a Transwell (Corning) until confluence was reached. Subsequently, green fluorescence cell tracker–labeled monocytes were added to the upper side of the Transwell, and pericyte-conditioned medium (PCM) from either the control or cocaine-exposed HBVPs was added to the lower chamber. Control PCM (without the cells) was incubated with 10 μM cocaine for 24 h and used as a negative control (CM-Cocaine) to eliminate any direct effect of cocaine on monocyte transmigration. Varying concentrations (25–100%) of conditioned medium incubated with cocaine were also added to the lower chamber of the Transwell and compared with conditioned medium collected from cocaine-treated and -untreated cultured pericytes. A dramatic increase in monocyte transmigration was observed in the presence of cocaine-treated PCM (PCM-cocaine) at all the concentrations tested compared with the PCM-Con (Fig. 8 B). Furthermore, we also sought to examine the transendothelial electrical resistance (TEER) and FITC Dextran-4 permeability of HBMECs following exposure to PCM-cocaine/PCM-Con/CM-cocaine. PCM-cocaine and PCM-Con at 50% concentration failed to exert any significant effect on TEER as well as permeability (Fig. S4, A and B). It was only at 100% concertation that PCM-cocaine showed significantly decreased TEER and increased permeability in the in vitro BBB model (Fig. S4, A and B).

Based on our findings that cocaine dose dependently increased CXCL10 expression in the culture medium of HBVPs (Fig. 2 G), we next sought to examine whether cocaine could also dose-dependently enhance monocyte transmigration across the BBB model. To address this, PCM was collected from HBVPs exposed to varying concentrations of cocaine (1, 10, and 100 μM)

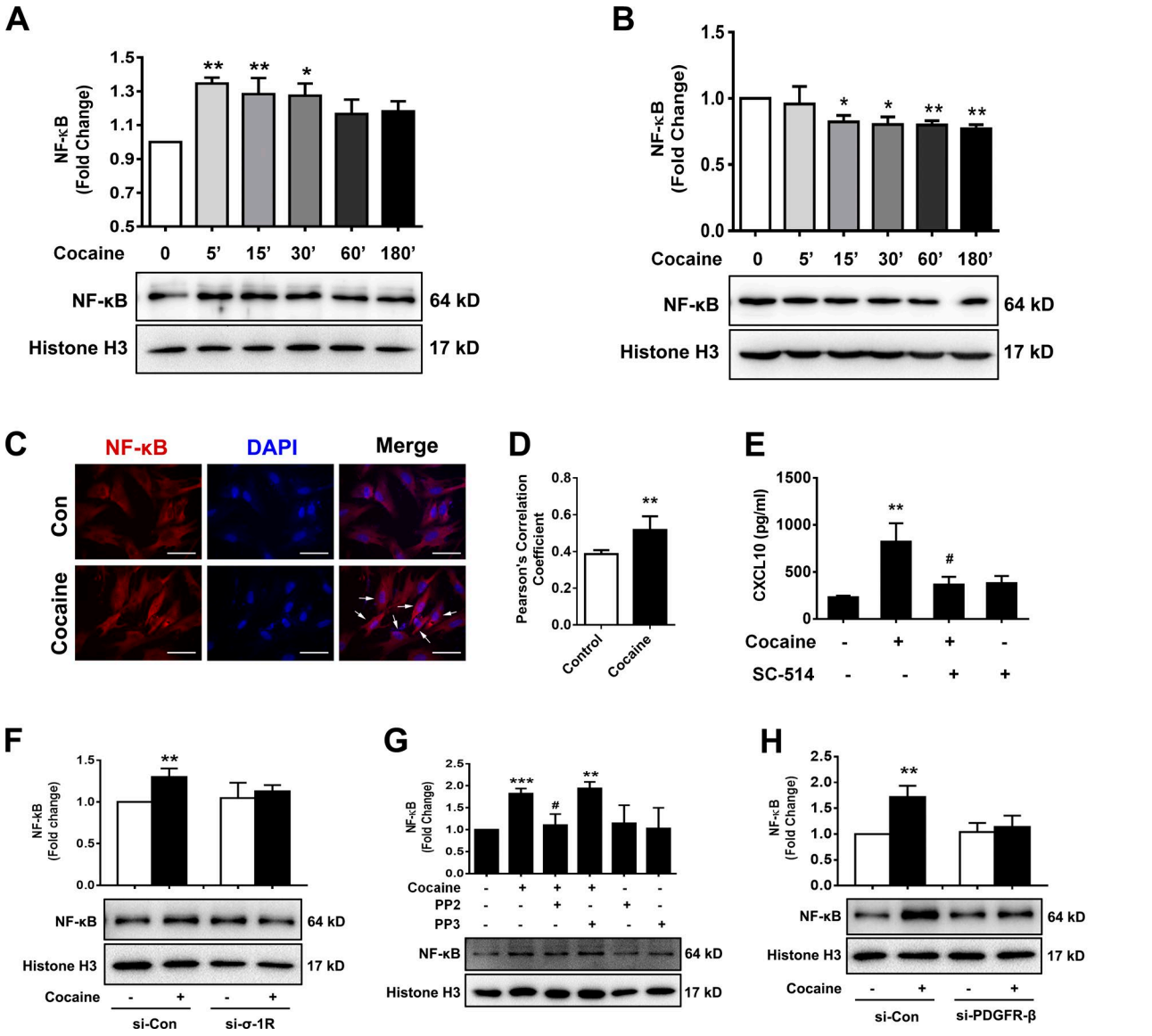

Figure 7. **Involvement of NF-κB in cocaine-mediated induction of CXCL10 release from HBVPs. (A)** Representative Western blot and quantification of NF-κB in the nuclear lysates isolated from HBVPs exposed to cocaine for various time points (5 min to 3 h). One-way ANOVA followed by Bonferroni's post hoc test was used to determine the statistical significance among multiple groups. **(B)** Representative Western blot and quantification of NF-κB in the cytoplasmic lysates isolated from HBVPs exposed to cocaine for various time points (5 min to 3 h). One-way ANOVA followed by Bonferroni's post hoc test was used to determine the statistical significance among multiple groups. **(C)** HBVPs were exposed to cocaine, followed by immunostaining with antibodies specific for NF-κB. Bars, 10 µm. White arrows, NF-κB nuclear translocated cells. **(D)** Quantification of NF-κB nuclear translocation. Two-tailed Student's *t* test. **(E)** CXCL10 was assayed by ELISA assay in the supernatants collected from HBVPs pretreated with IKK-2 inhibitor SC514 (10 µM) for 1 h, followed by cocaine exposure for an additional 24 h. One-way ANOVA followed by Bonferroni's post hoc test was used to determine the statistical significance among multiple groups. **(F)** Representative Western blot and quantification of NF-κB in the nuclear lysates isolated from HBVPs transfected with si–σ-1R and si-Con followed by cocaine exposure. Two-tailed Student's *t* test. **(G)** Representative Western blot and quantification of NF-κB in the nuclear lysates isolated from HBVPs pretreated with Src tyrosine kinase inhibitor PP2 or its inactive analogue PP3 for 1 h, followed by cocaine exposure for an additional 15 min. Two-tailed Student's *t* test. **(H)** Representative Western blot and quantification of NF-κB in the nuclear lysates isolated from HBVPs transfected with si–PDGFR-β and si-Con followed by cocaine exposure. Two-tailed Student's *t* test. All data are presented as means ± SD of three or four individual experiments (biological replicates). *, $P < 0.05$, **, $P < 0.01$, ***, $P < 0.001$ versus control group. #, $P < 0.05$ versus cocaine-treated group.

and assessed for its effect on monocyte transmigration across an in vitro BBB model. Control pericyte medium (without the cells) was incubated with 10 µM cocaine for 24 h and used as a negative control to eliminate any direct effect of cocaine on monocyte transmigration. Although control medium incubated with cocaine (10 µM) had the ability to induce a low level of monocyte transmigration, a more dramatic increase in monocyte transmigration was observed in the presence of PCM-cocaine, and this effect was dependent on the concentration of cocaine, with the maximal effect observed in PCM-cocaine (10 µM; Fig. 8 C). These findings thus demonstrate that PCM-cocaine enhanced monocyte transmigration compared with PCM-Con.

We next sought to examine whether CXCL10 released from HBVPs following cocaine exposure was a critical chemokine

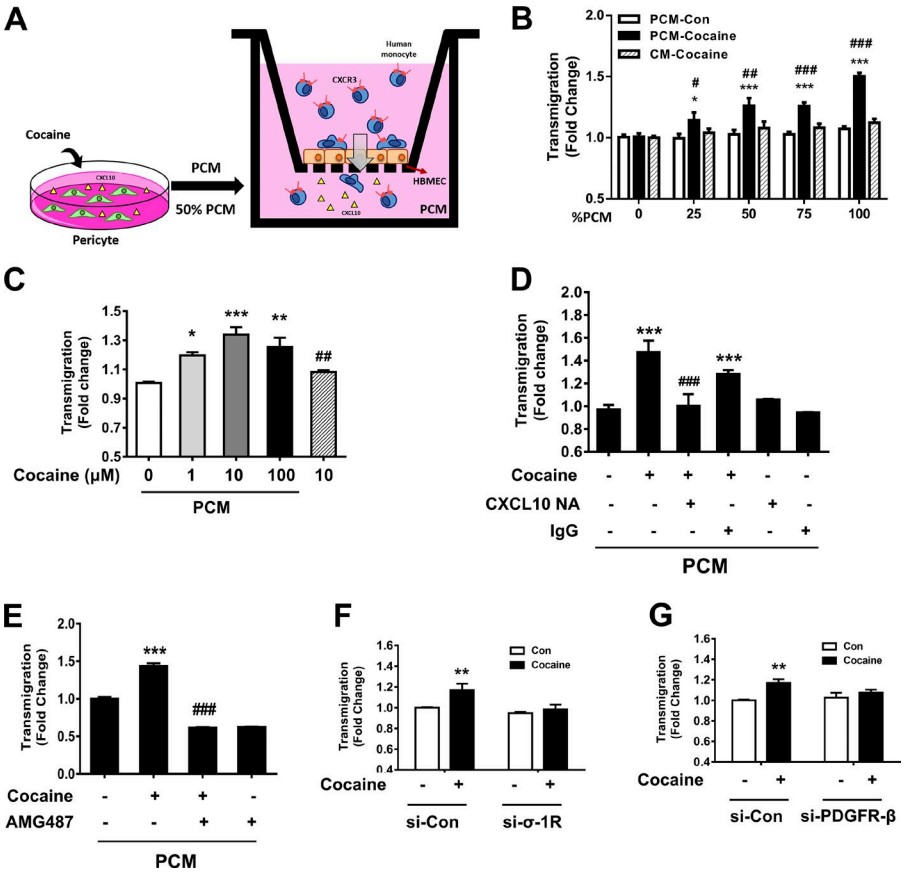

Figure 8. **Cocaine-mediated enhanced release of CXCL10 from HBVPs facilitated monocyte transmigration in an in vitro BBB model.** **(A)** Schematic of pericyte conditioned medium from HBVPs (PCM) collection and monocyte transmigration across the HBMECs. **(B)** Transmigration of monocytes exposed to different concentrations (25–100%) of PCM-Con, PCM-cocaine, or CM-cocaine in an in vitro BBB model. One-way ANOVA followed by Bonferroni's post hoc test was used to determine the statistical significance among multiple groups. *, P < 0.05, **, P < 0.01, ***, P < 0.001 versus 0% PCM group. #, P < 0.05, ##, P < 0.01, ###, P < 0.001 versus PCM-Con group. **(C)** PCM-cocaine induced transmigration of monocytes in a concentration-dependent manner. One-way ANOVA followed by Bonferroni's post hoc test was used to determine the statistical significance among multiple groups. *, P < 0.05, **, P < 0.01, ***, P < 0.001 versus PCM-Con group. ##, P < 0.01 versus PCM-cocaine (10 μM) group. **(D)** PCM-cocaine with neutralizing CXCL10 antibody failed to elicit monocyte transmigration, while control IgG antibody with PCM-cocaine induced monocyte transmigration. One-way ANOVA followed by Bonferroni's post hoc test was used to determine the statistical significance among multiple groups. ***, P < 0.001 versus PCM-Con group. ###, P < 0.001 versus PCM-cocaine group. **(E)** Pretreatment of monocytes with the CXCR3 antagonist AMG487 ameliorated PCM-cocaine induced monocyte transmigration. One-way ANOVA followed by Bonferroni's post hoc test was used to determine the statistical significance among multiple groups. ***, P < 0.001 versus PCM-Con group. ###, P < 0.001 versus PCM-cocaine group. **(F)** The PCM were collected from si–σ-1R or nonsense siRNA control transfected HBVPs, either unexposed or exposed to cocaine. PCM-cocaine induced monocyte transmigration was attenuated in the si–σ-1R transfected cells but not in the nonsense siRNA control group. Two-tailed Student's *t* test. **, P < 0.01 versus PCM-Con group. **(G)** PCM was collected from si–PDGFR-β or nonsense siRNA control transfected HBVPs either unexposed or exposed to cocaine. PCM-cocaine induced monocyte transmigration was attenuated in the si–PDGFR-β transfected group but not in the nonsense siRNA control group. Two-tailed Student's *t* test. **, P < 0.01 versus PCM-Con group. All data are presented as means ± SD of three or four individual experiments (biological replicates).

for enhanced monocyte transmigration. To answer this, PCM-Con and PCM-cocaine were incubated with either neutralizing anti-CXCL10 antibody or normal IgG antibody (2.0 μg/ml), followed by assessment of monocyte transmigration to these respective PCMs. PCM-cocaine incubated with neutralizing CXCL10 antibody failed to induce monocyte transmigration compared with PCM-cocaine incubated with the control IgG antibody, which resulted in enhanced monocyte transmigration (Fig. 8 D). To further confirm the effect of CXCL10 on monocyte transmigration, monocytes were pretreated with the CXCL10 receptor (CXCR3) antagonist AMG487 (1 μM) for 1 h and assessed as described before for transmigration across the BBB to either control or PCM-cocaine. Pretreatment of monocytes with AMG487 resulted in significant amelioration of PCM-cocaine to mediate monocyte transmigration. Control monocytes, not treated with the antagonist, exhibited increased migration to PCM-cocaine, as expected (Fig. 8 E).

Further validation of the involvement of σ-1R in PCM-cocaine–mediated transmigration of monocytes was performed in HBVPs transfected with the siRNA for σ-1R. Briefly, HBVPs were transfected with either σ-1R or nonsense (control) siRNA for 24 h followed by exposure of cells to cocaine for another 24 h, after which the PCM was collected and added to the bottom chamber of the Transwell. PCM-cocaine collected from HBVPs transfected with si–σ-1R failed to augment monocyte transmigration (Fig. 8 F). On the other hand, as expected, PCM-cocaine collected from HBVPs transfected with the nontarget siRNA control mediated an increase in monocyte transmigration. Next, we sought to examine the involvement of PDGFR-β in PCM-cocaine–mediated transmigration of monocytes by transfecting HBVPs with either control or si–PDGFR-β. HBVPs were transfected with either the PDGFR-β or nonsense (control) siRNA for 24 h followed by exposure of cells to cocaine for another 24 h, after which the PCM was collected and added to the bottom chamber of the Transwell for transmigration assays. PCM-cocaine collected from HBVPs transfected with si–PDGFR-β failed to augment monocyte transmigration, while, as expected, PCM-cocaine collected from HBVPs transfected with the nontarget siRNA control mediated an increase in monocyte transmigration (Fig. 8 G).

CXCL10 released from brain pericytes promoted monocyte transmigration in cocaine-treated mice

To further validate cocaine-mediated up-regulation of CXCL10 expression in pericytes in vivo, C57BL/6N mice (male, *n* = 4) were

injected with cocaine (20 mg/kg) or saline i.p. for 7 d, followed by assessment of the expression of CXCL10 in brain capillaries isolated from cocaine- versus saline-treated mice. MIVs were co-immunostained for pericyte marker (NG2, PDGFR-β, Desmin, or TBX18; red color) and CXCL10 (green color) and assessed by fluorescence microscopy. There was increased expression of CXCL10 in NG2$^+$ cells in MIVs isolated from cocaine-treated versus saline-treated mice (Fig. 9, A and B). Similar findings were observed in PDGFR-β$^+$, Desmin$^+$ or TBX18$^+$ cells in the MIVs (Fig. S5).

Based on the premise that pericyte coverage and vascular permeability are both important indicators of MIV functioning (Proebstl et al., 2012), we next sought to assess pericyte coverage and vascular permeability in MIVs from cocaine-treated mice. Brain sections from cocaine or saline-treated mice were costained with the pericyte markers (PDGFR-β or Desmin; red) and an endothelial cell marker (CD31; green). There was significantly decreased pericyte coverage in MIVs of mice administered cocaine compared with the saline group (Fig. S6). Brain sections from mice administered saline or cocaine were costained for fibrinogen, as well as the pericyte marker (Desmin) and endothelial cell marker (CD31), and quantified for perivascular fibrinogen leak. There was significantly increased fibrinogen leak in the brains of mice administered cocaine versus saline (Fig. S4 C).

Since CXCL10 expression was increased in cocaine-treated mice, we next wanted to validate the role of CXCL10 in monocyte transmigration in vivo. For this, C57BL/6N mice (male, n = 4) were administered either saline or CXCL10 (200 µg/ml, 4 µl) stereotactically at the coordinates +1.34 mm behind the bregma, +1.25 mm lateral from the sagittal midline at the depth of −4.0 mm to skull surface, followed 24 h later by tail vein injection of mouse bone marrow–derived monocytes (BMMs) isolated from CX3CR1–GFP mice. After an additional 24 h, animals were euthanized and brain sections stained with anti-GFP and anti-F4/80 antibodies. The cortex, hippocampus, thalamus, and striatal regions were assessed for distribution of F4/80$^+$ and GFP$^+$/F4/80$^+$ cells. Increased numbers of both F4/80$^+$ and GFP$^+$ and F4/80$^+$ cells were found in the hippocampi of mice administrated CXCL10 compared with the saline group (Fig. 9, C and D); similar findings were observed in the thalamus, cortex, and striatum of cocaine-treated mice (Fig. S7).

To validate the role of the monocyte CXCL10 receptor, CXCR3, in mediating monocyte transmigration, mice were injected with either saline or cocaine (20 mg/kg) for 7 d followed by tail vein injection of mouse BMMs isolated from CX3CR1-GFP mice pretreated with or without the CXCR3 antagonist AMG487. 24 h after the cell infusion, animals were euthanized, and brain sections were stained with anti-GFP, anti-F4/80, and anti-PDGFR-β antibodies. F4/80$^+$ as well as double-positive GFP$^+$/F4/80$^+$ cells in the cortex, hippocampus, thalamus, and striatum were quantified. In the presence of cocaine there were increased numbers of F4/80$^+$ as well as double-positive GFP$^+$/F4/80$^+$ cells in all the brain regions examined compared with the saline group (Fig. 9, E–L). In animals infused with BMMs isolated from CX3CR1-GFP mice that were pretreated with AMG487, cocaine failed to induce double-positive GFP$^+$/F4/80$^+$ cells, but not F4/80$^+$ cells, in all the brain regions examined.

Discussion

Cocaine abuse is closely linked with HIV infection (Dahal et al., 2015; Dash et al., 2015). Many studies have demonstrated an elevated risk of HIV acquisition and an enhanced progression to neurological HIV in cocaine abusers (Anthony et al., 1991; Chiasson et al., 1991; Doherty et al., 2000). Both cell culture and animal studies demonstrate that cocaine not only facilitates HIV replication in various cell types (Roth et al., 2002; Steele et al., 2003) but also results in glial cell activation, neurotoxicity, and BBB breakdown (Fiala et al., 1998; Gekker et al., 2006; Kousik et al., 2012). Cocaine has a detrimental effect on most cell types of the CNS, including the endothelium (Brailoiu et al., 2016), neurons (Mills et al., 2017), microglia (Liao et al., 2016), and astrocytes (Yang et al., 2010), likely underpinning the link between cocaine and HIV-associated neurocognitive impairment. Our findings add yet another novel role of pericytes in cocaine-mediated increased monocyte transmigration across the BBB. Here, we demonstrate a novel molecular mechanism underlying cocaine-mediated induction of CXCL10 expression in HBVPs, involving sequential activation and translocation of σ-1R, with subsequent interaction with c-Src, which in turn resulted in phosphorylation of PDGFR-β and nuclear translocation of NF-κB, leading ultimately to enhanced expression of CXCL10 (Fig. 10).

Pericytes are mural cells that are essential components of the microvascular vessels in direct contact with the endothelial cells (Sweeney et al., 2016). The integral role of pericytes in the development and maintenance of the cerebrovascular unit has been well recognized (Bergers and Song, 2005; Bell et al., 2010; Armulik et al., 2011), including regulation of the cerebral blood flow and neurovascular coupling (Kisler et al., 2017). Additionally, it has been reported that reduced coverage of pericytes on the endothelium can lead to MIV dysfunction and leakage (Sagare et al., 2013; Villaseñor et al., 2017). Whether these cells participate in inflammatory processes, however, remains poorly understood, especially in the context of cocaine-mediated brain inflammation. Herein, we provided evidence that in pericytes, cocaine mediates induction of the proinflammatory chemokine CXCL10 at both the transcriptional and post-transcriptional levels. CXCL10 belongs to the C-X-C chemokine family that binds to the G protein–coupled receptor CXCR3, and plays an important role in the chemotaxis of immune cells including T cells, monocytes, and NK cells (Taub et al., 1993). Increased expression of various chemokines in the CNS has been implicated in HIV-associated dementia (Sanders et al., 1998). Specifically, CXCL10 has been detected in the cerebrospinal fluid and brains of HIV-1–infected individuals (McArthur et al., 1993; Kolson and Pomerantz, 1996; Sanders et al., 1998; Kolb et al., 1999). In line with these findings, CXCL10 has also been identified as a plasma inflammatory biomarker signature of immune activation in HIV patients on antiretroviral therapy (Kamat et al., 2012). In the current study, we demonstrate that in HBVPs, cocaine exposure resulted in enhanced transcriptional regulation and stability of CXCL10 mRNA. We also showed that release of CXCL10 from cocaine-exposed pericytes was critical for transmigration of monocytes across the brain endothelium in both in vitro and in vivo model systems.

σ-1R is an intracellular molecular chaperone (28 kD) that is predominantly located in the ER membrane (Nguyen et al., 2015)

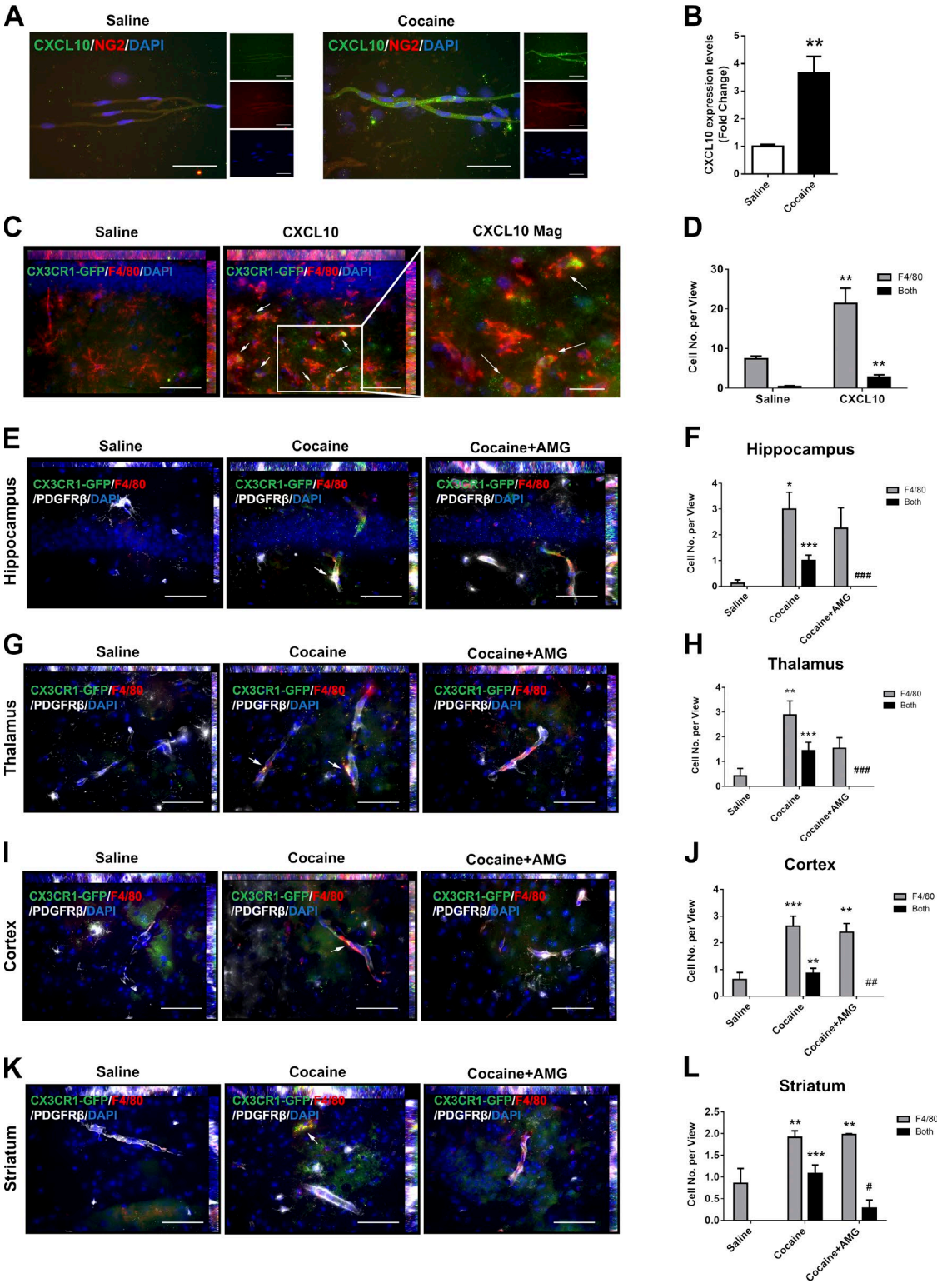

Figure 9. **CXCL10 released from pericytes promoted monocyte transmigration in mice administered cocaine. (A)** Double immunostaining of CXCL10 and pericyte marker NG2 in MIVs isolated from cocaine- or saline-treated mice. CXCL10, green; NG2, red; nucleus, blue; n = 4 per group; bar, 50 µm. **(B)** Quantification of the fluorescence intensity of CXCL10 in NG2$^+$ cells. Two-tailed Student's t test. **(C)** Representative images of F4/80$^+$ and GFP$^+$/F4/80$^+$ cells in the hippocampus of mice administrated saline or CXCL10. n = 4 per group. Arrow: GFP$^+$/F4/80$^+$ cells; bar, 50 µm; magnified images (mag), bar, 20 µm. **(D)** Quantification of F4/80$^+$ and double-positive GFP$^+$/F4/80$^+$ cells in the hippocampus of mice administrated saline or CXCL10. Two-tailed Student's t test. **(E)** Representative images of F4/80$^+$ and GFP$^+$/F4/80$^+$ cells in the hippocampus of mice administrated saline or cocaine that were costained with the pericyte marker PDGFR-β. AMG, AMG487. n = 4 per group. Arrow: GFP$^+$/F4/80$^+$ cells; bar, 50 µm. **(F)** Quantification of F4/80$^+$ and double-positive GFP$^+$/F4/80$^+$ cells in the hippocampi of mice administrated saline or cocaine. One-way ANOVA followed by Bonferroni's post hoc test was used to determine the statistical significance among multiple groups. **(G)** Representative images of F4/80$^+$ and GFP$^+$/F4/80$^+$ cells in the thalamus of mice administrated saline or cocaine that

and has been shown to bind to cocaine. It has also been implicated in cocaine addiction and toxicity (Yasui and Su, 2016). Intriguingly, as a target receptor for cocaine, several studies have also explored it as a therapeutic target for the treatment of cocaine-mediated neuropathology (Yasui and Su, 2016). Previous studies have shown that cocaine exacerbated neuroinflammation via activation of σ-1R in endothelial cells, astrocytes, and microglia (Yao et al., 2010, 2011b; Yang et al., 2015). Based on our previous findings, cocaine-mediated translocation of σ-1R increased the permeability of BBB (Yao et al., 2011b), induced chemokine monocyte chemotactic protein-1 (CCL2) in microglia (Yao et al., 2010), provoked transcription of GFAP (Yang et al., 2010), and exacerbated neurotoxicity mediated by HIV viral proteins (Yao et al., 2009). In the current study, we demonstrated that σ-1R was also present in the cytoplasm of pericytes and, in the presence of cocaine, it was found to translocate from the ER lipid droplets to the plasma membrane. Moreover, we observed that σ-1R activation was critical for cocaine-mediated induction of CXCL10 expression since pretreatment of HBVPs with the σ-1R antagonist BD1047 or in cells transfected with si–σ-1R, cocaine failed to induce induction of CXCL10.

Further dissection of the signaling pathways involved in cocaine-mediated induction of CXCL10 using pharmacological approaches revealed sequential activation of c-Src kinase, a finding that is consistent with previous reports on the effects of cocaine in HBMECs (Yao et al., 2011b). Herein, for the first time, we provide evidence that in HBVPs, cocaine mediates a direct physical interaction between σ-1R and c-Src. An interaction of σ-1R with c-Src was further confirmed by cotransfection of GFP-tagged c-Src and RFP-tagged σ-1R (σ-1R–RFP) plasmid constructs in HEK293 cells. Additionally, an interaction was validated by assessing endogenous levels of p-Src and σ-1R following cocaine stimulation in HBVPs by double immunostaining. Modulation of MAPKs by σ-1R has been reported by various investigators (Hayashi and Su, 2005; Yao et al., 2011b; Du et al., 2017). In the current study, using both pharmacological and genetic approaches, we demonstrated the role of σ-1R in cocaine-mediated phosphorylation of c-Src.

Our findings also suggest that drugs of abuse such as cocaine could directly phosphorylate cellular receptors such as PDGFR-β as early as 5 min. Further evaluation of the functional role of activated PDGFR-β was conducted using both pharmacological and genetic approaches. Pretreatment of HBVPs with either a receptor tyrosine kinase antagonist, such as STI571 or si–PDGFR-β, resulted in abrogation of cocaine-mediated induction of CXCL10 release from HBVPs, thereby implicating the role of PDGF signaling in this process. In this study, we found that cocaine-mediated phosphorylation of PDGFR-β was dependent on upstream activation of c-Src, since inhibition of Src kinase significantly blocked cocaine-mediated phosphorylation of PDGFR-β. Interestingly, inhibiting PDGFR-β had no effect on cocaine-induced activation of c-Src.

The transcription factor NF-κB has emerged as a major regulatory transcription factor for a number of genes, including cytokines such as CXCL10 (Fitzgerald et al., 2003; Krinninger et al., 2011). Our findings demonstrated a time-dependent translocation of NF-κB in HBVPs following cocaine stimulation. Further dissection of NF-κB regulation using both the pharmacological and genetic approaches revealed that NF-κB nuclear translocation was dependent on sequential activation of σ-1R, c-Src, and PDGFR-β signaling. It is likely that NF-κB, the downstream effector of the σ-1R–c-Src–PDGFR-β signaling, could also via feedback regulation mediate translocation of σ-1R as well as phosphorylation of downstream mediators such as c-Src and PDGFR-β. To investigate, we pretreated the cells with the IKK-2 inhibitor SC514 to block NF-κB nuclear translocation and demonstrated that NF-κB did not regulate the upstream σ-1R–c-Src–PDGFR-β signaling via the feedback regulation.

In the present study, we report an interaction of pericyte-released CXCL10 with monocytes, leading to increased transmigration of these latter cells in both in vitro as well as in vivo model systems. Our findings demonstrate that PCM derived from cocaine-treated HBVPs (PCM-cocaine) induced monocyte transmigration in a concentration-dependent manner. The direct effect of cocaine on monocyte transmigration was eliminated by using a negative control conditioned medium (without the HBVPs) incubated with cocaine (CM-cocaine). It was found that CM-cocaine induced monocyte transmigration only at 100% concentration, indicating thereby that cocaine itself had an effect on monocyte transmigration. PCM-cocaine, on the other hand, induced monocyte transmigration at all the concentrations tested (even as low as 25% concentration), demonstrating thereby that the chemokines released from cocaine-stimulated HBVPs had a stronger effect on monocyte transmigration. Additionally, we assessed TEER as well as BBB permeability in the in vitro model. PCM-cocaine as well as CM-cocaine were found to increase TEER while also decreasing the permeability of the in vitro BBB model, albeit only at 100% concentration. At lower concentrations (25–75%), however, only PCM-cocaine was able to induce monocyte transmigration. Intriguingly, there was not change in either TEER or BBB permeability in the presence of PCM-cocaine, demonstrating thereby that PCM-cocaine–mediated monocyte transmigration was unrelated to change in permeability. To attribute the specificity of CXCL10 in the PCM-cocaine as contributing to enhanced monocyte transmigration, PCM-cocaine

were costained with the pericyte marker PDGFR-β; $n = 4$ per group. Bar, 50 µm. **(H)** Quantification of F4/80$^+$ and GFP$^+$/F4/80$^+$ cells in the thalamus of mice administrated saline or cocaine. One-way ANOVA followed by Bonferroni's post hoc test was used to determine the statistical significance among multiple groups. **(I)** Representative images of F4/80$^+$ and GFP$^+$/F4/80$^+$ cells in the cortex of mice administrated saline or cocaine that were costained with the pericyte marker PDGFR-β. $n = 4$ per group. Bar, 50 µm. **(J)** Quantification of F4/80$^+$ and GFP$^+$/F4/80$^+$ cells in the cortex of mice administrated saline or cocaine. One-way ANOVA followed by Bonferroni's post hoc test was used to determine the statistical significance among multiple groups. **(K)** Representative images of F4/80$^+$ and double-positive GFP$^+$/F4/80$^+$ cells in the striatum of mice administrated saline or cocaine that were costained with the pericyte marker PDGFR-β. $n = 4$ per group. Bar, 50 µm. **(L)** Quantification of F4/80$^+$ and GFP$^+$/F4/80$^+$ cells in the striatum of mice administrated saline or cocaine. One-way ANOVA followed by Bonferroni's post hoc test was used to determine the statistical significance among multiple groups. *, $P < 0.05$, **, $P < 0.01$, ***, $P < 0.001$ versus saline group. #, $P < 0.05$, ##, $P < 0.01$, ###, $P < 0.001$ versus cocaine-treated group.

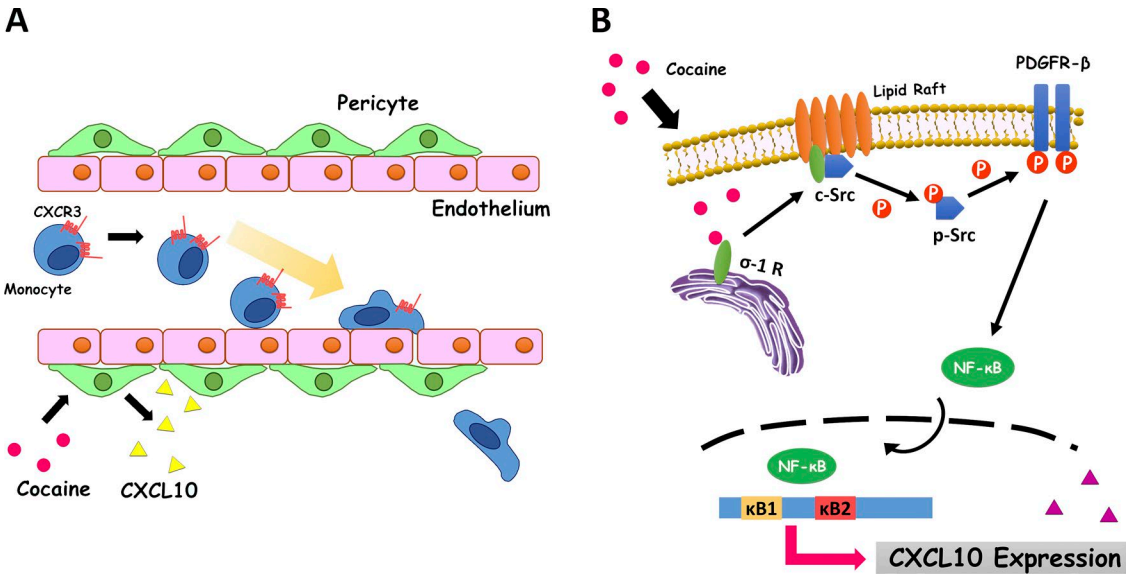

Figure 10. **Schematic diagram demonstrating signaling pathways involved in cocaine-mediated induction of CXCL10 expression in HBVPs.** **(A)** Cocaine-stimulated pericytes induce the expression and release of CXCL10, which in turn leads to enhanced monocyte transmigration across the BBB. **(B)** Cocaine-mediated σ-1R activation results in σ-1R translocation from ER to the plasma membrane with its subsequent interaction with c-Src. Activation of c-Src results in phosphorylation of PDGFR-β, leading, in turn, to nuclear translocation of NF-κB and subsequent CXCL10 expression. Increased CXCL10 ultimately leads to increased CXCR3-positive monocyte transmigration into the brain.

was treated with CXCL10 neutralizing antibody and assessed for monocyte migration. PCM-cocaine with was specifically able to block monocyte transmigration. Further validation of the role of CXCL10 and its signaling mediators in PCM-cocaine–mediated induction of monocyte transmigration was also determined by pharmacological and genetic approaches targeted at inactivation of σ-1R, PDGFR-β, and CXCR3 pathways.

To further unravel the effect of cocaine on CXCL10 induction in pericytes, MIVs from cocaine- or saline-treated mice were isolated and examined for expression of CXCL10 in pericytes. We observed increased localization of CXCL10 in NG2$^+$/PDGFR-β$^+$/Desmin$^+$/TBX18$^+$ pericytes in the MIVs isolated from cocaine-treated mice compared with vessels isolated form saline controls. Of note, four different pericyte markers were chosen to validate our findings. It should be mentioned that out of these markers, TBX18 is expressed in pericytes as well as vascular smooth muscle cells (Guimaraes-Camboa et al., 2017). Furthermore, in vivo validation of these findings also demonstrated that cocaine administration increased monocyte transmigration within the brain, and that this effect could be blocked in mice administered monocytes pretreated with the CXCR3 antagonist AMG487. These findings thus lend credence to a novel role of pericytes in cocaine-induced neuroinflammation mediated by CXCL10. Furthermore, we found increased fibrinogen leak and decreased pericyte coverage around the MIVs of mice administrated cocaine for 7 d, demonstrating thereby that cocaine increased the permeability of MIVs in vivo. Our findings are in agreement with previous reports describing the role of cocaine in mediating BBB breach (Sharma et al., 2009; Yao et al., 2011a). The interaction of pericytes with peripheral monocytes has ramifications for yet another novel mechanism by which cocaine abuse can exacerbate neuroinflammation specifically under conditions of HIV infection that are associated with BBB breach (Fiala et al., 1998; Napuri et al., 2013; Dahal et al., 2015).

In summary, our findings have delineated a detailed molecular pathway for cocaine-mediated induction of CXCL10 in pericytes with its ensuing effects causing exacerbation of neuroinflammation. Briefly, we have shown that cocaine-mediated induction of CXCL10 expression in HBVPs involves sequential activation and translocation of σ-1R with subsequent interaction of σ-1R with c-Src. Subsequent activation of c-Src leads to phosphorylation and activation of PDGFR-β, with downstream activation and nuclear translocation of NF-κB, leading ultimately to enhanced expression and release of CXCL10. Increased secretion of CXCL10, in turn, facilitates increased transmigration of monocytes across the BBB, thereby promoting enhanced inflammation in the brain. Strategies aimed at blocking cocaine-mediated signaling pathway could be developed as therapeutics to dampen cocaine-mediated neuroinflammation, with applications for other neurodegenerative disorders.

Materials and methods

Animals

C57BL/6 mice (male, 6–8 wk) were purchased from Charles River Laboratories, Inc. CX3CR1-GFP homozygous mice were obtained from the Jackson Laboratory and have a targeted deletion of CX3CR1 that is replaced by a GFP reporter insertion. All animals were housed under conditions of constant temperature and humidity on a 12-h light/12-h dark cycle, with lights on at 7:00 a.m. Food and water were available ad libitum. All animal procedures were performed according to the protocols approved by the Institutional Animal Care and Use Committee at the University of Nebraska Medical Center.

Cell culture

Primary HBVPs were purchased from ScienCell and cultured in the pericyte medium (ScienCell). HBVPs were isolated from fetal human brain and were positive for the pericyte markers PDGFR-β, NG2, Desmin, and TBX18. Pericytes had negligible staining for αSM as well as the endothelial cell marker CD31 (>98% purification; Fig. S1, A and B). Cell culture dishes were coated with poly-L-lysine (2 μg/cm^2; ScienCell), and cells were used in passages 2–5.

Primary HBMECs obtained from Dr. Monique Stins (Johns Hopkins University, Baltimore, MD) were cultured in RPMI 1640 medium (GE Healthcare Life Sciences) containing 10% heat-inactivated FBS (Atlanta Biologicals), 10% Nu-Serum (BD Biosciences), 2 mM L-glutamine (Invitrogen), 1 mM pyruvate (GE Healthcare Life Sciences), penicillin (100 U/ml), streptomycin (100 μg/ml; Gibco), essential amino acids (HyClone), and MEM vitamin solution (HyClone). Purified HBMECs were positive for endothelial makers DiI-AcLDL, ZO-1, and β-catenin and were found to be >99% pure after exclusion of staining for nonendothelial cell type markers (GFAP, smooth muscle actin, cytokeratin, and macrophage antigens), as described previously (Wen et al., 2011).

Monocyte isolation

Human monocytes were obtained from HIV-1, HIV-2, and hepatitis B seronegative donor leukopacks and separated by countercurrent centrifugal elutriation, as previously described (Gendelman et al., 1988). Freshly elutriated monocytes were cultured in DMEM (Gibco) containing 10% heat-inactivated human serum (Thermo Fisher Scientific), 2 mM L-glutamine (Invitrogen), 100 mg/ml gentamicin, and 10 mg/ml ciprofloxacin (Sigma-Aldrich). Human monocytes were used for the in vitro study, while BMMs isolated from mice were used for the in vivo study.

BMM isolation and cultivation

CX3CR1-GFP homozygous mice (Jackson Laboratory), 6–8 wk of age, were used as BMM donors. Briefly, the femur was removed, and bone marrow cells were dissociated into single-cell suspensions and were cultured for 5 d supplemented with 1,000 U/ml of macrophage colony-stimulating factor.

Reagents

Cocaine, σ-1R antagonist BD1047, IKK-2 inhibitor SC514, and FITC Dextran-4 were purchased from Sigma-Aldrich. Tyrosine kinase inhibitor STI571 was obtained from Novartis. Src kinase inhibitor (PP2) and its inactive orthologue (PP3) were purchased from Calbiochem. CXCR3 antagonist AMG487 was obtained from Tocris Bioscience. The concentrations of these inhibitors were based on the concentration curve study and our previous reports (Niu et al., 2014).

Cell Tracker Green 5-chloromethylfluorescein diacetate was purchased from Invitrogen. The human CXCL10/IP-10 DuoSet Kit was obtained from R&D Systems. CT-B conjugated to Alexa Fluor 488 was purchased from Invitrogen. Neutralizing human CXCL10/IP-10 antibody was purchased from R&D Systems.

RT-PCT and real-time PCR

The conditions for RT- and real-time PCR assays have been described previously (Niu et al., 2014). Real-time PCR primers for human CXCL10 and 18S were obtained from SA Biosciences. Total RNA was extracted with Trizol reagent (Invitrogen) according to the manufacturer's instructions. Quantitative analyses of mRNA were conducted using the ABI 7500 Fast Real-Time PCR system (Applied Biosystems). Real-time PCR amplifications were performed for 40 cycles (denaturation: 30 s at 95°C; annealing: 1 min at 60°C) and RT-PCR for 28 cycles (denaturation: 30 s at 94°C; annealing: 30 s at 55°C; extension: 30 s at 72°C). Primers were as follows: σ-1R, forward primer: 5′-CCCATGGGAACAAAT GAGACA-3′; reverse primer: 5′-CCAGATGGGTGTGAGTGCAT-3′; GAPDH (real-time PCR), forward primer: 5′-CTGTGGGCAAGG TCATCCCTG-3′; reverse primer: 5′-AGACGGCAGGTCAGGTCC ACC-3′; GAPDH (RT-PCR), forward primer: 5′-CGTGGAAGGACT CATGACCA-3′; reverse primer: 5′-GCCTGCTTCACCACCTTCTT-3′.

Collection of pericyte conditioned media

HBVPs at passages 3 and 4 were used for collection of PCM. For serum starvation, HBVP medium was replaced with FBS-free pericyte medium followed by overnight starvation and exposure to cocaine (10 μM). After 24-h incubation, PCM from PCM-Con– and PCM-cocaine–exposed groups were collected and centrifuged at 1,000 rpm for 5 min to remove cell debris. Collected supernatant was stored at −80°C until ready for use in transmigration assays.

Cytokine and chemokine analysis by Luminex

Supernatants were collected from HBVPs after 24 h of cocaine exposure, and the expression of cytokines/chemokines in supernatants was measured using the Milliplex MAP kit human Cytokine/Chemokine Magnetic Bead Panel Immunoassay (Millipore), which contains 29 different kinds of cytokines/chemokines as per the manufacturer's instructions. Briefly, this is a bead-based suspension array using the Luminex MAP technology in which fluorescent-coded beads have cytokine capture antibodies on the bead surface to bind the proteins. The heatmap was created by R version 3.2.3 software. Data represent results obtained from three biological replicates.

CXCL10 protein analysis by ELISA

Culture supernatants were collected from HBVPs exposed to cocaine or from untreated cells and assessed for expression of CXCL10 protein using a Human CXCL10/IP-10 DuoSet Kit (R&D Systems). Samples were analyzed for CXCL10 expression with three biological replicates, and each biological replicate had three or four technical replicates.

siRNA and plasmid transfection

HBVPs were transfected with siRNA of si-Con, si–σ-1R, or si–PDGFR-β (Thermo Fisher Scientific). The knockdown efficiency of siRNAs was determined by Western blot 1 d after transfection. HEK293 cells were cultured in the coverslip and cotransfected with plasmid constructs containing GFP-tagged c-Src and plasmid constructs containing σ-1R–RFP for 24 h followed by assessment of colocalization of GFP-tagged c-Src and σ-1R–RFP using an inverted LSM 700 confocal microscope with a 40× oil objective (Zeiss). Images were processed with the Zeiss Zen microscope software.

Luciferase assay

The 972-bp full-length CXCL10 promoter construct, the 376-bp truncated CXCL10 promoter construct (sequence from −279 to +97), and point mutations in the putative AP-1, κB1, κB2, and ISRE recognition elements in the 972-bp full-length CXCL10 promoter were provided by Dr. David Proud.

HBVPs were transfected with the following luciferase reporter plasmids: full-length CXCL10, truncated CXCL10, AP-1 mut, κB1 mut, κB2 mut, or ISRE mut CXCL10 promoter plasmids. For normalization of transfection efficiencies, cells were also cotransfected with pRL-TK plasmid DNA containing the *Renilla* luciferase gene. 24 h after transfection, cells were treated with or without cocaine for 4 h, followed by assessed the luciferase activity using the Dual-Luciferase Reporter Assay System (Promega) according to the manufacturer's instructions. Data represent results obtained from three biological replicates, and each biological replicate comprised three technical replicates.

mRNA stability assays

For mRNA stability assays, 10 µg/ml Act D (Sigma-Aldrich) was added to HBVPs cultured in the presence or absence of cocaine (10 µM) for 30, 60, 90, 120, and 180 min. At selected times following Act D treatment, total RNA was harvested, and CXCL10 mRNA expression was detected by real-time RT-PCR. The fold change in gene expression determined from the RT-PCR assay was then used to calculate the percentage of mRNA remaining following Act D treatment. Data represent results obtained from three biological replicates, and each biological replicate comprised three technical replicates.

Lipid raft isolation and analysis

Lipid rafts were isolated from confluent HBVPs treated with or without cocaine according to a previous study (Yao et al., 2011b). Briefly, lysates were mixed with 1 ml of 85% (wt/vol) sucrose and overlaid with 2 ml of 42.5% sucrose, 6 ml of 35% sucrose, and 6 ml and 5 ml of 5% sucrose. The gradient was centrifuged for 24 h at 39,000 rpm (SW 41 rotor; Beckman) at 4°C. 12 fractions were harvested from top to bottom (900 µl–1 ml per fraction) and frozen at −80°C until analysis. The concentration of protein in each fraction was analyzed with a bicinchoninic acid protein assay kit (Pierce).

Labeling of the lipid rafts

CT-B conjugated to Alexa Fluor 488, which binds the ganglioside GM1 (a lipid raft marker), was used to label the lipid rafts. It has been known that CT-B colocalizes with flotillin, a protein that is known to be located in lipid rafts and ceramide. HBVPs were cultured onto coverslips and transfected with σ-1R–RFP plasmid for 24 h, followed by exposure to cocaine (10 µM) for 30 min at 37°C. CT-B conjugated to Alexa Fluor 488 (1 ng/ml) was added to the HBVPs during the last 10 min of incubation. The coverslips were then washed three times with ice-cold PBS, fixed with ice-cold 4% paraformaldehyde, and mounted with mounting medium (Prolong Gold Anti-fade Reagent; Invitrogen). Fluorescent images were acquired at RT on a Zeiss Observer using a Z1 inverted microscope with a 63×/1.4 oil-immersion objective. Images were processed using the AxioVs 40 Version 4.8.0.0 software (Zeiss). Data represent results obtained from three biological replicates, and each biological replicate comprised three technical replicates.

Western blot

Treated cells or isolated MIVs were lysed using the Mammalian Cell Lysis kit (Sigma-Aldrich), as described previously (Niu et al., 2014). Equal amounts of protein were electrophoresed in a SDS-polyacrylamide gel under reducing conditions followed by transfer to PVDF membranes. Blots were blocked with 5% BSA in TBS-Tween, and Western blots were probed with antibodies specific for σ-1R (15168-I-AP; Proteintech Group), Src (2108; Cell Signaling), p-PDGFR-β (3161; Cell Signaling), NG2 antibodies (ab129051; Abcam), TBX18 (ab115262; Abcam), αSM (A5228; Sigma-Aldrich), and histone H3 (9715; Cell Signaling) at 1:1,000 dilution; NF-κB (ab16502; Abcam) at 1:2,000 dilution; ganglioside GM1 (bs-2367R; One World Lab) at 1:500 dilution; and p-Src (ab32078; Abcam), PDGFR-β (ab32570; Abcam), Desmin (ab32362; Abcam), and β-actin (A5316; Sigma-Aldrich) at 1:5,000 dilution. Secondary antibodies were alkaline phosphatase conjugated to goat anti-mouse/rabbit IgG, or rabbit anti-goat IgG (1:10,000; Jackson ImmunoResearch Labs). Signals were detected by SuperSignal West Dura Extended Duration or Pico PLUS Chemiluminescent Substrate (Thermo Fisher Scientific). All experiments had at least four biological replicates, and representative blots are presented in the figures.

Immunoprecipitation

To investigate the interaction between c-Src with σ-1R, HBVPs were treated with cocaine (10 µM) for different time periods (5, 15, and 30 min) and then lysed in RIPA buffer (50 mM Tris, pH 7.4, 150 mM NaCl, 5 mM EDTA, pH 8.0, 0.1% SDS, 1.0% NP-40, and 0.5% sodium deoxycholate) containing proteinase and phosphatase inhibitors. Cellular protein (500 µg) was incubated with c-Src antibody (1:100; 2108; Cell Signaling) overnight at 4°C and precipitated with protein A/G beads (Santa Cruz Biotechnology). The mixture was then centrifuged at 12,000 rpm for 1 min, and the cell pellets were rinsed twice with the lysis buffer (1.0% NP-40, 0.5% sodium deoxycholate, 0.1% SDS, 150 mM NaCl, 9.1 mM Na_2HPO_4, and 1.7 mM NaH_2PO_4) containing proteinase and phosphatase inhibitors. Finally, 30 µl of 2× Western blot loading buffer was added and boiled for 5 min. The protein complexes were detected using σ-1R antibody, while the input protein (without antibody addition) served as a control to show that equal amounts of total protein were used. To confirm the interaction of these two proteins, the σ-1R antibody (2 µg/150 µg total protein; sc-13705; Santa Cruz Biotechnology) was used to pull down the protein, and c-Src antibody was used to detect the signal.

To investigate the phosphorylation of PDGFR-β, HBVPs were treated with cocaine (10 µM) for various times and then lysed using RIPA buffer. For each sample, 150 µg of protein was used for immunoprecipitation. Cell lysates were incubated with 1 µl of anti-4G10 antibody (05-1050; Millipore) overnight at 4°C followed by the same procedure, as described above. Finally, 30 µl of 2× Western blot loading buffer was added and boiled for 5 min. After spinning at 12,000 rpm for 1 min, the supernatants were subjected to Western blot analysis and detected by p-PDGFR-β

antibody, while the input protein (without antibody addition) served as a control to show that equal amounts of total protein were used. Data represent results obtained from three biological replicates, and representative blots are presented in the figures.

Monocyte transmigration assay in vitro

Boyden chambers (Corning Costar) were used to determine the transmigration of monocytes in vitro. Briefly, primary HBMECs were seeded (4×10^4 cells/well) onto 6.5-mm polyester Transwell inserts (3-µm pore size) and grown for 5 d to achieve confluence. Human monocytes were fluorescently labeled with 10 µM cell tracker green for 10 min at 37°C. Labeled cells (10^6 cells/ml) were added to the upper compartment of Transwell inserts in serum-free medium, while PCM was added to the basal side of the chamber. The Transwell plates were incubated for 18 h at 37°C, followed by quantification of monocyte transmigration by measuring the number of cells migrating across the insert with a Synergy Mx fluorescence plate reader (BioTek Instruments). Data represent results obtained from three biological replicates, and each biological replicate comprised two or three technical replicates.

Cell permeability assay

Primary HBMECs were seeded (4×10^4 cells/well) onto 6.5-mm polyester Transwell inserts (3-µm pore size) and grown for 5 d to achieve confluence. HBMEC monolayers were exposed to varying concentrations (50%–100%) of PCM-Con or PCM-cocaine for 18 h. FITC Dextran-4 (100 ng/ml) was then added to the upper chamber of the inserts and incubated for an additional 2 h. Aliquots (100 µl) were then collected from the lower chamber for measurement of fluorescence at 480 and 530 nm wavelengths for excitation and emission, respectively (BioTek Instruments). Permeability changes were expressed as fluorescence intensity of FITC-Dextran transported across the BBB into the lower chamber compared with PCM-Con. Data represent results obtained from three biological replicates, and each biological replicate comprised two or three technical replicates.

Isolation of brain MIVs

Brain MIVs were isolated as described previously (Niu et al., 2014). Briefly, the brains were removed and immediately immersed in ice-cold isolation buffer A (103 mM NaCl, 4.7 mM KCl, 2.5 mM $CaCl_2$, 1.2 mM KH_2PO_4, 1.2 mM $MgSO_4$, and 15 mM Hepes, pH 7.4). The choroid plexus, meninges, cerebellum, and brain stem were removed followed by homogenization of the brain in 2.5 ml of isolation buffer B (25 mM $NaHCO_3$, 10 mM glucose, 1 mM Na^+ pyruvate, and 10 g/liter dextran, pH 7.4) with complete protease inhibitors. 6 ml of Dextran (26%) was then added to the homogenates followed by centrifugation at 5,800 *g* for 20 min. Cell pellets were resuspended in isolation buffer B and filtered through a 70-µm mesh filter (Becton Dickinson). Filtered homogenates were repelleted by centrifugation, and part of it was used for staining by smearing on glass slides.

Immunofluorescence staining

Brain MIVs smeared on glass slides and HBVP cultured on coverslips were fixed with 4% formaldehyde in PBS for 20 min at RT. The slides or coverslips were washed three times with PBS, permeabilized with 0.3% Triton X-100 for 30 min, rewashed three times, and blocked in 10% goat serum in PBS for 2 h at RT. The following antibodies were used for immunostaining: p-Src (1:100; ab32078; Abcam), σ-1R (1:100; sc-137075; Santa Cruz Biotechnology), NF-κB (1:100; ab16502; Abcam), CXCL10 (1:50; ab8098; Abcam), NG2 (1:200; ab129051; Abcam), PDGFR-β (1:100; ab32570; Abcam), Desmin (1:50; ab32362; Abcam), TBX18 (1:100; ab115262; Abcam), and CD31 (1:500; NB600-1475; Novus). The slides or coverslips were washed with PBS and incubated with Alexa Fluor 594–conjugated anti-mouse or anti-rabbit, Alexa Fluor 488–conjugated anti-rabbit or anti-mouse, Alexa Fluor 488–conjugated anti-mouse, or Alexa Fluor 594–conjugated anti-rabbit immunoglobulin G (Invitrogen) for 1 h at RT. After a final washing with PBS, the slides or coverslips were mounted with mounting medium (Prolong Gold Antifade Reagent; Invitrogen). Fluorescent images were acquired at RT on a Zeiss Observer, using a Z1 inverted microscope with a 40×/1.3 or 63×/1.4 oil-immersion objective. Images were processed with the AxioVs 40 Version 4.8.0.0 software (Zeiss). Photographs were acquired with an AxioCam MRm digital camera and were analyzed with ImageJ software.

Tissue source and Immunofluorescence staining

Formalin-fixed, paraffin-embedded sections (5 µm) of frontal cortex from normal individuals or cocaine abusers were obtained from the Douglas-Bell Canada Brain Bank (see Table S1 for clinical data) and stained with antibodies specific for CD68 (1:100; ab955; Abcam), TMEM119 (1:100; ab185333; Abcam), and Desmin (10 µg/ml; AF3844; R&D Systems) overnight at 4°C. Frozen frontal cortex tissues with the same identification number were also obtained from the Douglas-Bell Canada Brain Bank and used for MIV isolations. Isolated MIVs were costained with anti-CXCL10 (1:50; ab8098; Abcam) and antibodies specific for pericyte markers (PDGFR-β [1:100; ab32570; Abcam], NG2 [1:200; ab129051; Abcam], Desmin [1:50; ab32362; Abcam], or TBX18 [1:100; ab115262; Abcam]) and CD31 (1:500; NB600-1475; Novus) overnight at 4°C. Brain sections or isolated MIVs were washed three times in PBS followed by incubation in Alexa Fluor 594–conjugated anti-mouse or anti-rabbit, Alexa Fluor 488–conjugated anti-rabbit or anti-mouse, and Alexa Fluor 647–conjugated anti-goat or anti-rat immunoglobulin G (Invitrogen) for 2 h at RT. After a final washing with PBS, sections were mounted with the mounting medium. Fluorescent images were acquired at RT on a Zeiss Observer using a Z1 inverted microscope with a 40×/1.3 or 63×/1.4 oil-immersion objective. Z-stacks were generated from images taken at 0.50–0.8-µm intervals. Images were processed using the AxioVs 40 Version 4.8.0.0 software (Zeiss). Photographs were acquired with an AxioCam MRm digital camera and were analyzed with ImageJ software. $CD68^+/TMEM119^-$ cells proximal to $Desmin^+$ MIVs were counted. For MIVs, only those with a diameter <6 µm were used for quantification (Halliday et al., 2016).

Stereotaxic injection

8-wk-old C57BL/6N mice (male, $n = 4$) were microinjected with either saline (200 ng/µl) or CXCL10 (4 µl) into the brain using the microinjection parameters (coordinates +1.34 mm behind the

bregma, +1.25 mm lateral from the sagittal midline at the depth of −4.0 mm to skull surface; flow rate: 0.5 µl/min). After 1 h, animals were injected with BMMs isolated from CX3CR1-GFP mice at a concentration of 10^7 cells/100 µl through the tail vein. 24 h after cell infusion, the animals were euthanized and subjected to transcranial perfusion with saline to remove CX3CR1-GFP$^+$ monocytes from tissue blood vessels. Brain tissues were removed and frozen at −80°C until cryosection. Sections were then stained with anti-GFP (1:500; ab13970; Abcam) and anti-F4/80 (1:100; ab6640; Abcam) antibodies and subjected to immunostaining as described above. Using four animals per group, different regions of the mouse brains were then quantified for double-positive cells in the cortex, hippocampus, thalamus, and striatum regions. For MIVs, only those with a diameter <6 µm were used for quantification (Halliday et al., 2016).

In vivo monocyte transmigration assay

Assay of monocyte transmigration into the brain was performed in C57BL/6 mice. Animals were divided into three groups (n = 4): (1) saline, (2) cocaine, and (3) cocaine plus AMG487 (1 µM). Cocaine was injected once daily at a dose of 20 mg/kg intraperitoneally for 7 d. On the eighth day, animals were injected with BMMs isolated from CX3CR1-GFP mice with or without pretreatment of AMG487 at a concentration of 10^7 cells/100 µl through the tail vein. 24 h after cell infusion, the animals were euthanized and subjected to transcranial perfusion with saline to remove CX3CR1-GFP$^+$ monocytes from tissue blood vessels. Brain tissues were removed and frozen at −80°C until cryosection. Brain sections were then stained with GFP (1:500; ab13970; Abcam), F4/80 (1:100; ab6640; Abcam), and PDGFR-β (1:100; ab32570; Abcam), following the immunostaining protocol described above. Labeled cells were then quantified in the different regions including cortex, hippocampus, thalamus, and striatum. Only vessels with a diameter <6 µm were considered as MIVs (Halliday et al., 2016).

Pericyte coverage and fibrinogen leakage

C57BL/6 mice were divided into two groups (n = 4): (1) saline and (2) cocaine. Cocaine was injected once daily at a dose of 20 mg/kg intraperitoneally for 7 d, and then animals were euthanized and subjected to transcranial perfusion with saline to remove blood from tissue blood vessels. Brain tissues were removed and frozen at −80°C until cryosection. Brain sections were stained with anti-fibrinogen (1:50; ab34269; Abcam) and/or antibodies specific for pericyte markers (PDGFR-β [1:100; ab32570; Abcam] or Desmin [1:100; ab8976; Abcam] and CD31 [1:500; NB600-1475; Novus]) overnight at 4°C. Brain sections were washed three times in PBS followed by incubation with Alexa Fluor 594–conjugated anti-mouse or anti-rabbit, Alexa Fluor 488–conjugated anti-rabbit or anti-rat, or Alexa Fluor 647–conjugated anti-rat immunoglobulin G (Invitrogen) for 2 h at RT. After a final washing with PBS, sections were mounted with the mounting medium. Fluorescent images were acquired at RT on a Zeiss Observer by a Z1 inverted microscope with a 40×/1.3 or 20×/0.8 oil-immersion objective. Z-stacks were generated from images taken at 0.50–0.8-µm intervals. Images were processed using the AxioVs 40 Version 4.8.0.0 software (Zeiss). Photographs were acquired with an AxioCam MRm digital camera and were analyzed with ImageJ software. For MIVs, only those with a diameter <6 µm were used for quantification for both pericyte coverage and fibrinogen leakage, which were described previously (Mehla et al., 2012; Nikolakopoulou et al., 2017). Briefly, for pericyte coverage, the percentage of Desmin- or PDGFR-β–positive surface area covering CD31$^+$ capillary surface area was quantified. For fibrinogen leakage, the perivascular fibrinogen signals on the abluminal side of MIVs were analyzed.

Statistical analysis

Statistical analysis was performed using a two-tailed Student's t test for comparison of the two groups and one-way ANOVA with a Bonferroni's post hoc test for multiple comparisons. For comparison between the two groups, an F test was used to determine the equality of variances between groups. For comparison among multiple groups, a Brown-Forsythe test was used to determine the equality of variances among groups. Results were judged statistically significant if $P < 0.05$ by ANOVA for both Student's t test and one-way ANOVA test. Data distribution was assumed to be normal, but this was not formally tested.

Online supplemental material

Table S1 shows clinical data for human brain tissue samples. Fig. S1 shows immunostaining of different cell markers in HBVPs and MTS assay of cell viability of HBVPs. Fig. S2 shows CXCL10 mRNA expression levels in HEK293 cells and representative Western blots of σ-1R in 10 lipid raft isolation fractions. Fig. S3 shows pretreatment of HBVPs with the IKK-2/NF-κB inhibitor SC514 failed to abrogate cocaine-mediated lipid raft translocation of σ-1R, Src phosphorylation, and PDGFR-β phosphorylation. Fig. S4 shows the effect of cocaine on permeability of BBB in vitro and in vivo. Fig. S5 shows CXCL10 expression levels in pericytes of MIVs isolated from brains of mice administrated either saline or cocaine. Fig. S6 shows pericyte coverage in MIVs from brains of mice administrated either saline or cocaine. Fig. S7 shows CX3CR1-GFP$^+$ BMMs transmigration in the brain of mice administrated CXCL10.

Acknowledgments

We thank the Douglas-Bell Canada Brain Bank for providing the frozen and formalin-fixed brain samples of cocaine abusers; Dr. David Proud for providing all the luciferase reporter plasmids—full-length CXCL10, truncated CXCL10, AP-1 mut, κB1 mut, κB2 mut, or ISRE mut CXCL10 promoter plasmids; Dr. Naoto Yamaguchi (Chiba University, Chiba, Japan) for providing the GFP-tagged c-Src plasmid; and Dr. Tsung Ping Su (National Institute on Drug Abuse, Bethesda, MD) for providing us with the σ-1R–RFP plasmid.

This work was supported by National Institutes of Health, National Institute on Drug Abuse grants DA035203, DA040397, DA041751, DA044586 (to S. Buch); DA043138 (to S. Buch and G. Hu); and DA046831 and DA042704 (to G. Hu); and National Institute of Mental Health grants MH106425 (to S. Buch) and MH112848 (to S. Buch and G. Hu), as well as the Nebraska Center for Substance Abuse Research. The project was supported by National Institutes of Health, National Institute of Mental Health

grant 2P30MH062261. The content is solely the responsibility of the authors and does not necessarily represent the official views of the National Institutes of Health.

The authors declare no competing financial interests.

Author contributions: F. Niu, G. Hu, and S. Buch designed the research; F. Niu, K. Liao, S. Sil, M. Guo, and L. Yang performed research; and F. Niu, G. Hu, K. Liao, S. Callen, and S. Buch wrote the manuscript.

Submitted: 8 December 2017
Revised: 28 August 2018
Accepted: 8 November 2018

References

Anthony, J.C., D. Vlahov, K.E. Nelson, S. Cohn, J. Astemborski, and L. Solomon. 1991. New evidence on intravenous cocaine use and the risk of infection with human immunodeficiency virus type 1. *Am. J. Epidemiol.* 134:1175–1189. https://doi.org/10.1093/oxfordjournals.aje.a116021

Armulik, A., G. Genové, and C. Betsholtz. 2011. Pericytes: developmental, physiological, and pathological perspectives, problems, and promises. *Dev. Cell.* 21:193–215. https://doi.org/10.1016/j.devcel.2011.07.001

Bell, R.D., E.A. Winkler, A.P. Sagare, I. Singh, B. LaRue, R. Deane, and B.V. Zlokovic. 2010. Pericytes control key neurovascular functions and neuronal phenotype in the adult brain and during brain aging. *Neuron.* 68:409–427. https://doi.org/10.1016/j.neuron.2010.09.043

Bergers, G., and S. Song. 2005. The role of pericytes in blood-vessel formation and maintenance. *Neuro-oncol.* 7:452–464. https://doi.org/10.1215/S1152851705000232

Bodmer, M., F. Enzler, E. Liakoni, M. Bruggisser, and M.E. Liechti. 2014. Acute cocaine-related health problems in patients presenting to an urban emergency department in Switzerland: a case series. *BMC Res. Notes.* 7:173. https://doi.org/10.1186/1756-0500-7-173

Brailoiu, G.C., E. Deliu, L.M. Console-Bram, J. Soboloff, M.E. Abood, E.M. Unterwald, and E. Brailoiu. 2016. Cocaine inhibits store-operated Ca2+ entry in brain microvascular endothelial cells: critical role for sigma-1 receptors. *Biochem. J.* 473:1–5. https://doi.org/10.1042/BJ20150934

Butoi, E.D., A.M. Gan, I. Manduteanu, D. Stan, M. Calin, M. Pirvulescu, R.R. Koenen, C. Weber, and M. Simionescu. 2011. Cross talk between smooth muscle cells and monocytes/activated monocytes via CX3CL1/CX3CR1 axis augments expression of pro-atherogenic molecules. *Biochim. Biophys. Acta.* 1813:2026–2035. https://doi.org/10.1016/j.bbamcr.2011.08.009

Chiasson, M.A., R.L. Stoneburner, D.S. Hildebrandt, W.E. Ewing, E.E. Telzak, and H.W. Jaffe. 1991. Heterosexual transmission of HIV-1 associated with the use of smokable freebase cocaine (crack). *AIDS.* 5:1121–1126. https://doi.org/10.1097/00002030-199109000-00011

Cinque, P., A. Bestetti, R. Marenzi, S. Sala, M. Gisslen, L. Hagberg, and R.W. Price. 2005. Cerebrospinal fluid interferon-gamma-inducible protein 10 (IP-10, CXCL10) in HIV-1 infection. *J. Neuroimmunol.* 168:154–163. https://doi.org/10.1016/j.jneuroim.2005.07.002

Corrêa, J.D., D. Starling, A.L. Teixeira, P. Caramelli, and T.A. Silva. 2011. Chemokines in CSF of Alzheimer's disease patients. *Arq. Neuropsiquiatr.* 69:455–459. https://doi.org/10.1590/S0004-282X2011000400009

Dahal, S., S.V. Chitti, M.P. Nair, and S.K. Saxena. 2015. Interactive effects of cocaine on HIV infection: implication in HIV-associated neurocognitive disorder and neuroAIDS. *Front. Microbiol.* 6:931. https://doi.org/10.3389/fmicb.2015.00931

Dash, S., M. Balasubramaniam, F. Villalta, C. Dash, and J. Pandhare. 2015. Impact of cocaine abuse on HIV pathogenesis. *Front. Microbiol.* 6:1111. https://doi.org/10.3389/fmicb.2015.01111

Dhillon, N.K., R. Williams, F. Peng, Y.J. Tsai, S. Dhillon, B. Nicolay, M. Gadgil, A. Kumar, and S.J. Buch. 2007. Cocaine-mediated enhancement of virus replication in macrophages: implications for human immunodeficiency virus-associated dementia. *J. Neurovirol.* 13:483–495. https://doi.org/10.1080/13550280701528684

Doherty, M.C., R.S. Garfein, E. Monterroso, D. Brown, and D. Vlahov. 2000. Correlates of HIV infection among young adult short-term injection drug users. *AIDS.* 14:717–726. https://doi.org/10.1097/00002030-200004140-00011

Du, K., X. Wang, L. Chi, and W. Li. 2017. Role of Sigma-1 Receptor/p38 MAPK Inhibition in Acupoint Catgut Embedding-Mediated Analgesic Effects in Complete Freund's Adjuvant-Induced Inflammatory Pain. *Anesth. Analg.* 125:662–669. https://doi.org/10.1213/ANE.0000000000001857

Fiala, M., X.H. Gan, L. Zhang, S.D. House, T. Newton, M.C. Graves, P. Shapshak, M. Stins, K.S. Kim, M. Witte, and S.L. Chang. 1998. Cocaine enhances monocyte migration across the blood-brain barrier. Cocaine's connection to AIDS dementia and vasculitis? *Adv. Exp. Med. Biol.* 437:199–205. https://doi.org/10.1007/978-1-4615-5347-2_22

Filion, L.G., G. Graziani-Bowering, D. Matusevicius, and M.S. Freedman. 2003. Monocyte-derived cytokines in multiple sclerosis. *Clin. Exp. Immunol.* 131:324–334. https://doi.org/10.1046/j.1365-2249.2003.02053.x

Fitzgerald, K.A., D.C. Rowe, B.J. Barnes, D.R. Caffrey, A. Visintin, E. Latz, B. Monks, P.M. Pitha, and D.T. Golenbock. 2003. LPS-TLR4 signaling to IRF-3/7 and NF-kappaB involves the toll adapters TRAM and TRIF. *J. Exp. Med.* 198:1043–1055. https://doi.org/10.1084/jem.20031023

Fox, H.C., C. D'Sa, A. Kimmerling, K.M. Siedlarz, K.L. Tuit, R. Stowe, and R. Sinha. 2012. Immune system inflammation in cocaine dependent individuals: implications for medications development. *Hum. Psychopharmacol.* 27:156–166. https://doi.org/10.1002/hup.1251

Gekker, G., S. Hu, W.S. Sheng, R.B. Rock, J.R. Lokensgard, and P.K. Peterson. 2006. Cocaine-induced HIV-1 expression in microglia involves sigma-1 receptors and transforming growth factor-beta1. *Int. Immunopharmacol.* 6:1029–1033. https://doi.org/10.1016/j.intimp.2005.12.005

Gendelman, H.E., J.M. Orenstein, M.A. Martin, C. Ferrua, R. Mitra, T. Phipps, L.A. Wahl, H.C. Lane, A.S. Fauci, D.S. Burke, et al. 1988. Efficient isolation and propagation of human immunodeficiency virus on recombinant colony-stimulating factor 1-treated monocytes. *J. Exp. Med.* 167:1428–1441. https://doi.org/10.1084/jem.167.4.1428

Grozdanov, V., C. Bliederhaeuser, W.P. Ruf, V. Roth, K. Fundel-Clemens, L. Zondler, D. Brenner, A. Martin-Villalba, B. Hengerer, J. Kassubek, et al. 2014. Inflammatory dysregulation of blood monocytes in Parkinson's disease patients. *Acta Neuropathol.* 128:651–663. https://doi.org/10.1007/s00401-014-1345-4

Guimaraes-Camboa, N., P. Cattaneo, Y. Sun, T. Moore-Morris, Y. Gu, N.D. Dalton, E. Rockenstein, E. Masliah, K.L. Peterson, W.B. Stallcup, et al. 2017. Pericytes of Multiple Organs Do Not Behave as Mesenchymal Stem Cells In Vivo. *Cell Stem Cell.* 20:345–359.e5. https://doi.org/10.1016/j.stem.2016.12.006

Hall, C.N., C. Reynell, B. Gesslein, N.B. Hamilton, A. Mishra, B.A. Sutherland, F.M. O'Farrell, A.M. Buchan, M. Lauritzen, and D. Attwell. 2014. Capillary pericytes regulate cerebral blood flow in health and disease. *Nature.* 508:55–60. https://doi.org/10.1038/nature13165

Halliday, M.R., S.V. Rege, Q. Ma, Z. Zhao, C.A. Miller, E.A. Winkler, and B.V. Zlokovic. 2016. Accelerated pericyte degeneration and blood-brain barrier breakdown in apolipoprotein E4 carriers with Alzheimer's disease. *J. Cereb. Blood Flow Metab.* 36:216–227. https://doi.org/10.1038/jcbfm.2015.44

Hayashi, T., and T.P. Su. 2003. Intracellular dynamics of sigma-1 receptors (sigma(1) binding sites) in NG108-15 cells. *J. Pharmacol. Exp. Ther.* 306:726–733. https://doi.org/10.1124/jpet.103.051292

Hayashi, T., and T.P. Su. 2005. The potential role of sigma-1 receptors in lipid transport and lipid raft reconstitution in the brain: implication for drug abuse. *Life Sci.* 77:1612–1624. https://doi.org/10.1016/j.lfs.2005.05.009

Ioannidis, L.J., C.Q. Nie, A. Ly, V. Ryg-Cornejo, C.Y. Chiu, and D.S. Hansen. 2016. Monocyte- and Neutrophil-Derived CXCL10 Impairs Efficient Control of Blood-Stage Malaria Infection and Promotes Severe Disease. *J. Immunol.* 196:1227–1238. https://doi.org/10.4049/jimmunol.1501562

Kamat, A., V. Misra, E. Cassol, P. Ancuta, Z. Yan, C. Li, S. Morgello, and D. Gabuzda. 2012. A plasma biomarker signature of immune activation in HIV patients on antiretroviral therapy. *PLoS One.* 7:e30881. https://doi.org/10.1371/journal.pone.0030881

Kisler, K., A.R. Nelson, S.V. Rege, A. Ramanathan, Y. Wang, A. Ahuja, D. Lazic, P.S. Tsai, Z. Zhao, Y. Zhou, et al. 2017. Pericyte degeneration leads to neurovascular uncoupling and limits oxygen supply to brain. *Nat. Neurosci.* 20:406–416. https://doi.org/10.1038/nn.4489

Koetzler, R., R.S. Zaheer, S. Wiehler, N.S. Holden, M.A. Giembycz, and D. Proud. 2009. Nitric oxide inhibits human rhinovirus-induced transcriptional activation of CXCL10 in airway epithelial cells. *J. Allergy Clin. Immunol.* 123:201–208.e9. https://doi.org/10.1016/j.jaci.2008.09.041

Kolb, S.A., B. Sporer, F. Lahrtz, U. Koedel, H.W. Pfister, and A. Fontana. 1999. Identification of a T cell chemotactic factor in the cerebrospinal fluid of HIV-1-infected individuals as interferon-gamma inducible protein 10. *J. Neuroimmunol.* 93:172–181. https://doi.org/10.1016/S0165-5728(98)00223-9

Kolson, D.L., and R.J. Pomerantz. 1996. AIDS Dementia and HIV-1-Induced Neurotoxicity: Possible Pathogenic Associations and Mechanisms. *J. Biomed. Sci.* 3:389–414.

Kousik, S.M., T.C. Napier, and P.M. Carvey. 2012. The effects of psychostimulant drugs on blood brain barrier function and neuroinflammation. *Front. Pharmacol.* 3:121. https://doi.org/10.3389/fphar.2012.00121

Krauthausen, M., M.P. Kummer, J. Zimmermann, E. Reyes-Irisarri, D. Terwel, B. Bulic, M.T. Heneka, and M. Müller. 2015. CXCR3 promotes plaque formation and behavioral deficits in an Alzheimer's disease model. *J. Clin. Invest.* 125:365–378. https://doi.org/10.1172/JCI66771

Krinninger, P., C. Brunner, P.A. Ruiz, E. Schneider, N. Marx, A. Foryst-Ludwig, U. Kintscher, D. Haller, H. Laumen, and H. Hauner. 2011. Role of the adipocyte-specific NF-κB activity in the regulation of IP-10 and T cell migration. *Am. J. Physiol. Endocrinol. Metab.* 300:E304–E311. https://doi.org/10.1152/ajpendo.00143.2010

Lane, B.R., S.R. King, P.J. Bock, R.M. Strieter, M.J. Coffey, and D.M. Markovitz. 2003. The C-X-C chemokine IP-10 stimulates HIV-1 replication. *Virology.* 307:122–134. https://doi.org/10.1016/S0042-6822(02)00045-4

Lepej, S.Z., L. Misić-Majerus, T. Jeren, O.D. Rode, A. Remenar, V. Sporec, and A. Vince. 2007. Chemokines CXCL10 and CXCL11 in the cerebrospinal fluid of patients with tick-borne encephalitis. *Acta Neurol. Scand.* 115:109–114. https://doi.org/10.1111/j.1600-0404.2006.00726.x

Li, C.-S.R. 2016. Cerebral gray matter volumes in cocaine dependence: clinical and functional implications. *In* Neuropathology of Drug Addictions and Substance Misuse. Vol. 2. V.R. Preedy, editor. Academic Press, New York. 245–256. https://doi.org/10.1016/B978-0-12-800212-4.00024-8

Liao, K., M. Guo, F. Niu, L. Yang, S.E. Callen, and S. Buch. 2016. Cocaine-mediated induction of microglial activation involves the ER stress-TLR2 axis. *J. Neuroinflammation.* 13:33. https://doi.org/10.1186/s12974-016-0501-2

Majlesi, N., R. Shih, F.W. Fiesseler, O. Hung, and R. Debellonio. 2010. Cocaine-associated seizures and incidence of status epilepticus. *West. J. Emerg. Med.* 11:157–160.

McArthur, J.C., D.R. Hoover, H. Bacellar, E.N. Miller, B.A. Cohen, J.T. Becker, N.M. Graham, J.H. McArthur, O.A. Selnes, L.P. Jacobson, et al. 1993. Dementia in AIDS patients: incidence and risk factors. Multicenter AIDS Cohort Study. *Neurology.* 43:2245–2252. https://doi.org/10.1212/WNL.43.11.2245

Mehla, R., S. Bivalkar-Mehla, M. Nagarkatti, and A. Chauhan. 2012. Programming of neurotoxic cofactor CXCL-10 in HIV-1-associated dementia: abrogation of CXCL-10-induced neuro-glial toxicity in vitro by PKC activator. *J. Neuroinflammation.* 9:239. https://doi.org/10.1186/1742-2094-9-239

Mendoza, R., B.L. Miller, and I. Mena. 1992. Emergency room evaluation of cocaine-associated neuropsychiatric disorders. Vol. 10. Recent Developments in Alcoholism. Springer Verlag, New York. https://doi.org/10.1007/978-1-4899-1648-8_4

Mills, F., A.K. Globa, S. Liu, C.M. Cowan, M. Mobasser, A.G. Phillips, S.L. Borgland, and S.X. Bamji. 2017. Cadherins mediate cocaine-induced synaptic plasticity and behavioral conditioning. *Nat. Neurosci.* 20:540–549. https://doi.org/10.1038/nn.4503

Napuri, J., S. Pilakka-Kanthikeel, A. Raymond, M. Agudelo, A. Yndart-Arias, S.K. Saxena, and M. Nair. 2013. Cocaine enhances HIV-1 infectivity in monocyte derived dendritic cells by suppressing microRNA-155. *PLoS One.* 8:e83682. https://doi.org/10.1371/journal.pone.0083682

Nguyen, L., B.P. Lucke-Wold, S.A. Mookerjee, J.Z. Cavendish, M.J. Robson, A.L. Scandinaro, and R.R. Matsumoto. 2015. Role of sigma-1 receptors in neurodegenerative diseases. *J. Pharmacol. Sci.* 127:17–29. https://doi.org/10.1016/j.jphs.2014.12.005

Nikolakopoulou, A.M., Z. Zhao, A. Montagne, and B.V. Zlokovic. 2017. Regional early and progressive loss of brain pericytes but not vascular smooth muscle cells in adult mice with disrupted platelet-derived growth factor receptor-β signaling. *PLoS One.* 12:e0176225. https://doi.org/10.1371/journal.pone.0176225

Niu, F., H. Yao, W. Zhang, R.L. Sutliff, and S. Buch. 2014. Tat 101-mediated enhancement of brain pericyte migration involves platelet-derived growth factor subunit B homodimer: implications for human immunodeficiency virus-associated neurocognitive disorders. *J. Neurosci.* 34:11812–11825. https://doi.org/10.1523/JNEUROSCI.1139-14.2014

Park, I.W., J.F. Wang, and J.E. Groopman. 2001. HIV-1 Tat promotes monocyte chemoattractant protein-1 secretion followed by transmigration of monocytes. *Blood.* 97:352–358. https://doi.org/10.1182/blood.V97.2.352

Pirvulescu, M.M., A.M. Gan, D. Stan, V. Simion, M. Calin, E. Butoi, and I. Manduteanu. 2014. Subendothelial resistin enhances monocyte transmigration in a co-culture of human endothelial and smooth muscle cells by mechanisms involving fractalkine, MCP-1 and activation of TLR4 and Gi/o proteins signaling. *Int. J. Biochem. Cell Biol.* 50:29–37. https://doi.org/10.1016/j.biocel.2014.01.022

Proebstl, D., M.B. Voisin, A. Woodfin, J. Whiteford, F. D'Acquisto, G.E. Jones, D. Rowe, and S. Nourshargh. 2012. Pericytes support neutrophil subendothelial cell crawling and breaching of venular walls in vivo. *J. Exp. Med.* 209:1219–1234. https://doi.org/10.1084/jem.20111622

Rhoney, D.H. 2010. Stroke. *In* Drug-Induced Diseases: Prevention, Detection, and Management. D.A. James, and E.M. Tisdale, editors. American Society of Health-System Pharmacists, Bethesda, MD. 190–204.

Roth, M.D., D.P. Tashkin, R. Choi, B.D. Jamieson, J.A. Zack, and G.C. Baldwin. 2002. Cocaine enhances human immunodeficiency virus replication in a model of severe combined immunodeficient mice implanted with human peripheral blood leukocytes. *J. Infect. Dis.* 185:701–705. https://doi.org/10.1086/339012

Rutledge, C.A., F.S. Ng, M.S. Sulkin, I.D. Greener, A.M. Sergeyenko, H. Liu, J. Gemel, E.C. Beyer, A.A. Sovari, I.R. Efimov, and S.C. Dudley. 2014. c-Src kinase inhibition reduces arrhythmia inducibility and connexin43 dysregulation after myocardial infarction. *J. Am. Coll. Cardiol.* 63:928–934. https://doi.org/10.1016/j.jacc.2013.10.081

Sagare, A.P., R.D. Bell, Z. Zhao, Q. Ma, E.A. Winkler, A. Ramanathan, and B.V. Zlokovic. 2013. Pericyte loss influences Alzheimer-like neurodegeneration in mice. *Nat. Commun.* 4:2932. https://doi.org/10.1038/ncomms3932

Sanders, V.J., C.A. Pittman, M.G. White, G. Wang, C.A. Wiley, and C.L. Achim. 1998. Chemokines and receptors in HIV encephalitis. *AIDS.* 12:1021–1026. https://doi.org/10.1097/00002030-199809000-00009

Sharma, H.S., D. Muresanu, A. Sharma, and R. Patnaik. 2009. Cocaine-induced breakdown of the blood-brain barrier and neurotoxicity. *Int. Rev. Neurobiol.* 88:297–334. https://doi.org/10.1016/S0074-7742(09)88011-2

Simmons, R.P., E.P. Scully, E.E. Groden, K.B. Arnold, J.J. Chang, K. Lane, J. Lifson, E. Rosenberg, D.A. Lauffenburger, and M. Altfeld. 2013. HIV-1 infection induces strong production of IP-10 through TLR7/9-dependent pathways. *AIDS.* 27:2505–2517. https://doi.org/10.1097/01.aids.0000432455.06476.bc

Sørensen, T.L., F. Sellebjerg, C.V. Jensen, R.M. Strieter, and R.M. Ransohoff. 2001. Chemokines CXCL10 and CCL2: differential involvement in intrathecal inflammation in multiple sclerosis. *Eur. J. Neurol.* 8:665–672. https://doi.org/10.1046/j.1468-1331.2001.00327.x

Steele, A.D., E.E. Henderson, and T.J. Rogers. 2003. Mu-opioid modulation of HIV-1 coreceptor expression and HIV-1 replication. *Virology.* 309:99–107. https://doi.org/10.1016/S0042-6822(03)00015-1

Stephens, B.G., J.M. Jentzen, S. Karch, D.C. Mash, and C.V. Wetli. 2004. Criteria for the interpretation of cocaine levels in human biological samples and their relation to the cause of death. *Am. J. Forensic Med. Pathol.* 25:1–10. https://doi.org/10.1097/01.paf.0000118960.58334.a9

Substance Abuse and Mental Health Services Administration (SAMHSA), Center for Behavioral Health Statistics and Quality (CBHSQ). 2013. Drug Abuse Warning Network, 2011: National Estimates of Drug-Related Emergency Department Visits. SAMHSA, Rockville, MD. Available at: https://www.samhsa.gov/data/sites/default/files/DAWN2k11ED/DAWN2k11ED/DAWN2k11ED.pdf/.

Substance Abuse and Mental Health Services Administration, Center for Behavioral Health Statistics and Quality. 2013. The DAWN Report: Highlights of the 2011 Drug Abuse Warning Network (DAWN). Findings on Drug-Related Emergency Department Visits, Rockville, MD. https://www.samhsa.gov/data/sites/default/files/DAWN2k11ED/DAWN2k11ED/DAWN2k11ED.pdf.

Sweeney, M.D., S. Ayyadurai, and B.V. Zlokovic. 2016. Pericytes of the neurovascular unit: key functions and signaling pathways. *Nat. Neurosci.* 19:771–783. https://doi.org/10.1038/nn.4288

Taub, D.D., A.R. Lloyd, K. Conlon, J.M. Wang, J.R. Ortaldo, A. Harada, K. Matsushima, D.J. Kelvin, and J.J. Oppenheim. 1993. Recombinant human interferon-inducible protein 10 is a chemoattractant for human monocytes and T lymphocytes and promotes T cell adhesion to endothelial cells. *J. Exp. Med.* 177:1809–1814. https://doi.org/10.1084/jem.177.6.1809

Thériault, P., A. ElAli, and S. Rivest. 2015. The dynamics of monocytes and microglia in Alzheimer's disease. *Alzheimers Res. Ther.* 7:41. https://doi.org/10.1186/s13195-015-0125-2

United Nations Office on Drugs and Crime. 2016. World Drug Report. Vol. Sales No. E. 16. XI. 7. United Nations Publication, Vienna, Austria. Available at: http://www.unodc.org/doc/wdr2016/WORLD_DRUG_REPORT_2016_web.pdf.

Vargas-Inchaustegui, D.A., A.E. Hogg, G. Tulliano, A. Llanos-Cuentas, J. Arevalo, J.J. Endsley, and L. Soong. 2010. CXCL10 production by human

monocytes in response to Leishmania braziliensis infection. *Infect. Immun.* 78:301–308. https://doi.org/10.1128/IAI.00959-09

Villaseñor, R., B. Kuennecke, L. Ozmen, M. Ammann, C. Kugler, F. Gruninger, H. Loetscher, P.O. Freskgard, and L. Collin. 2017. Region-specific permeability of the blood-brain barrier upon pericyte loss. *J. Cereb. Blood Flow Metab.* 37:3683–3694. https://doi.org/10.1177/0271678X17697340

Wen, H., Y. Lu, H. Yao, and S. Buch. 2011. Morphine induces expression of platelet-derived growth factor in human brain microvascular endothelial cells: implication for vascular permeability. *PLoS One.* 6:e21707. https://doi.org/10.1371/journal.pone.0021707

Yang, L., H. Yao, X. Chen, Y. Cai, S. Callen, and S. Buch. 2015. Role of Sigma Receptor in Cocaine-Mediated Induction of Glial Fibrillary Acidic Protein: Implications for HAND. *Mol. Neurobiol.* 53:1329–1342. https://doi.org/10.1007/s12035-015-9094-5

Yang, Y., H. Yao, Y. Lu, C. Wang, and S. Buch. 2010. Cocaine potentiates astrocyte toxicity mediated by human immunodeficiency virus (HIV-1) protein gp120. *PLoS One.* 5:e13427. https://doi.org/10.1371/journal.pone.0013427

Yao, H., J.E. Allen, X. Zhu, S. Callen, and S. Buch. 2009. Cocaine and human immunodeficiency virus type 1 gp120 mediate neurotoxicity through overlapping signaling pathways. *J. Neurovirol.* 15:164–175. https://doi.org/10.1080/13550280902755375

Yao, H., Y. Yang, K.J. Kim, C. Bethel-Brown, N. Gong, K. Funa, H.E. Gendelman, T.P. Su, J.Q. Wang, and S. Buch. 2010. Molecular mechanisms involving sigma receptor-mediated induction of MCP-1: implication for increased monocyte transmigration. *Blood.* 115:4951–4962. https://doi.org/10.1182/blood-2010-01-266221

Yao, H., M. Duan, and S. Buch. 2011a. Cocaine-mediated induction of platelet-derived growth factor: implication for increased vascular permeability. *Blood.* 117:2538–2547. https://doi.org/10.1182/blood-2010-10-313593

Yao, H., K. Kim, M. Duan, T. Hayashi, M. Guo, S. Morgello, A. Prat, J. Wang, T.P. Su, and S. Buch. 2011b. Cocaine hijacks σ1 receptor to initiate induction of activated leukocyte cell adhesion molecule: implication for increased monocyte adhesion and migration in the CNS. *J. Neurosci.* 31:5942–5955. https://doi.org/10.1523/JNEUROSCI.5618-10.2011

Yasui, Y., and T.P. Su. 2016. Potential Molecular Mechanisms on the Role of the Sigma-1 Receptor in the Action of Cocaine and Methamphetamine. *J. Drug Alcohol. Res.* 5:235970. https://doi.org/10.4303/jdar/235970

Zajkowska, J., A. Moniuszko-Malinowska, S.A. Pancewicz, A. Muszyńska-Mazur, M. Kondrusik, S. Grygorczuk, R. Swierzbińska-Pijanowska, J. Dunaj, and P. Czupryna. 2011. Evaluation of CXCL10, CXCL11, CXCL12 and CXCL13 chemokines in serum and cerebrospinal fluid in patients with tick borne encephalitis (TBE). *Adv. Med. Sci.* 56:311–317. https://doi.org/10.2478/v10039-011-0033-z